

**CHARACTERIZATION OF *THERMOBIFIDA FUSCA* CELLULASE
ACTIVITY ON UNNATURAL CELLULOSE ALLOMORPHS**

By

YUXIN LIU

A thesis submitted to the

School of Graduate Studies

Rutgers, The State University of New Jersey

In partial fulfillment of the requirements

For the degree of

Master of Science

Graduate Program in Chemical and Biochemical Engineering

Written under the direction of

Dr. Shishir P. S. Chundawat

And approved

New Brunswick, New Jersey

[October, 2018]

ABSTRACT OF THESIS

Characterization of *T. fusca* cellulase activity on unnatural cellulose allomorphs

By Yuxin Liu

Thesis Director:

Dr. Shishir Chundawat

Cellulases have traditionally been studied in the context of cellulose degradation to fermentable sugars, like glucose, for ethanol production. Cellulose recalcitrance to enzymatic degradation has long been considered as a critical technological barrier for commercialization of cellulosic biofuels. Recent research has led to the development of a cost-effective ammonia-based pretreatment method that allows modification of the crystalline allomorphic structure of cellulose from native cellulose-I to cellulose-III.^{*} Chundawat and co-workers have already demonstrated that cellulose-III is up to five folds more digestible than native cellulose I by *Trichoderma reesei* derived fungal cellulase enzymes.[†] This improvement in fungal cellulase cocktail activity was shown to be largely arising due to enhanced endolytic-exolytic cellulase enzyme synergy on pretreated cellulose-III. Here, we explore the activity of cellulases secreted by a highly cellulolytic actinomycete called *Thermobifida fusca*. To the best of our knowledge, the work here signifies the first reported attempt to characterize the activity of *T. fusca* expressed cellulase cocktails and purified bacterial cellulases on pretreated cellulose-III. The four specific objectives that were completed to accomplish this goal were; (i) develop and optimize a cell culturing method for *T. fusca* growth to maximize recovered cellulase activity, (ii) characterize the activity of isolated crude *T. fusca* cellulase cocktails on native and ammonia-pretreated cellulose allomorphs, (iii) develop a protein purification protocol to isolate

^{*} da Costa Sousa, L. et al. Next-generation ammonia pretreatment enhances cellulosic biofuel production. *Energy Environ. Sci.* 9, 1215–1223 (2016).

[†] Chundawat, S. P. S. et al. Restructuring the crystalline cellulose hydrogen bond network enhances its depolymerization rate. *J. Am. Chem. Soc.* 133, 11163–11174 (2011).

and purify *T. fusca* exocellulase (Cel6B) to electrophoretic homogeneity, and (iv) run enzyme synergism ‘re-start’ hydrolysis assays on isolated exocellulase Cel6B in concert with another bacterial endocellulase (CelE) to confirm if bacterial cellulases also show improved endo-exo synergistic activity on cellulose-III. Our results led further credence to our initial hypothesis that free cellulolytic enzyme cocktails, derived from either fungal or bacterial sources, show enhanced endo-exo synergy on pretreated cellulose-III. We also discuss future research directions and the relevance of the research to our understanding about how cellulases deconstruct various crystalline cellulose allomorphs in general.

ACKNOWLEDGEMENTS

I would firstly like to thank my parents, for their trust, love and patience during the past three years, their financial support and passionate encouragement that made it possible for me to complete this project. I also submit my heartiest gratitude to my thesis advisor, Dr. Shishir Chundawat, for his sincere guidance and invaluable suggestions with this project. I would like to thank Dr. Zhang and Dr. Pedersen for serving on my committee. I would like to thank all staff members at the Department of Chemical and Biochemical Engineering (Rutgers University) for their supportive help. I am also very grateful for having great laboratory colleagues; their love has made it possible for me to have another family in the U.S. I am especially thankful to Bhargava Nemmaru for his help and patience. I also acknowledge the help of Amenah Soherwardy and Haiyan Zheng for their help with performing mass spectrometry and proteomics data analysis. Special thanks to Dr. Yongling Qin for helping set up *T. fusca* cell culture experiments in the initial phase of the project. Finally, I would like to thank the National Science Foundation (NSF Award 1604421) and Rutgers University (SOE Start-up Fund) for supporting this research project.

Table of Contents

ABSTRACT OF THESIS	ii
ACKNOWLEDGEMENTS	iv
Chapter 1. Introduction	1
1.1 Research background	1
1.2 Aims of the project:	4
Chapter 2. Optimization of <i>T.fusca</i> growth conditions to maximize enzyme production	5
2.1 Materials and Methods	5
2.1.1 Cell culturing and sample preparation	5
2.1.2 Assays used for determination of protein concentration and activity of cellulases	7
2.1.3 Expression and purification of CelE and CelE-CBM3a	9
2.2 Results	10
2.2.1 Screen of carbon source and growth time on cellulases expression	10
2.2.2 Screen of growth temperature and pH	15
2.3 Discussion	17
Chapter 3 Purification of Cel6B	20
3.1 Materials and methods	20
3.1.1 Ammonium sulfate saturation of the culture broth	20
3.1.2 Dialysis or desalting chromatography	21
3.1.3 Ion-Exchange (IEX) chromatography	22
3.1.4 Size Exclusion chromatography	23
3.1.5 Activity assays for eluted FPLC protein fractions	24
3.1.6 LC-MS identification of proteins from SDS-PAGE	26
3.2 Results	27
3.2.1 Optimization of ammonium sulfate saturation concentration	27
3.2.2 Ion-Exchange chromatography purification of Cel6B and other cellulases	29
3.2.3 Size exclusion chromatography polishing of Cel6B	32
3.2.4 Activity assay results	33
3.2.5 LC-MS/MS proteomics analysis to validate Cel6B and other cellulase fractions	36
3.3 Discussion	40
Chapter 4 Activity assays	46
4.1 Materials and methods	46
4.1.1 Crude enzyme assays	46
4.1.2 Purified Cel6B activity assays	48
4.1.3 Synergism assay on CI and CIII	49
4.2 Result	50
4.2.1 Crude enzyme assays result	50
4.2.2 Purified Cel6B assay	52
4.2.3 CelE and CelE-CBM3a binding and activity to create endo-cuts on cellulose	54
4.2.4 Synergism assay with Cel6B	58

4.3 Discussion	59
Chapter 5. Future Studies and Conclusions	62

List of figures

Figure 1. Impact of anhydrous liquid ammonia pretreatment on cellulose allomorphic structures.	2
Figure 2. Protein concentration profile of fermentation broth of <i>T. fusca</i> grown on different carbon sources and at various growth time points.	10
Figure 3. Protein concentration profile of fermentation cell pellets of <i>T. fusca</i> grown on different carbon sources and at various growth time points.	11
Figure 4. pNPC cellulase activity detected in <i>T. fusca</i> broth at various fermentation time points.	11
Figure 5. <i>T. fusca</i> culture broths highlighting expressed total proteins/enzymes for different carbon sources at various time points.	14
Figure 6. Bradford assay results <i>T. fusca</i> protein expressed in broth at various temperatures and pHs.	16
Figure 7. pNPC activity assay results of optimization of cell culture growth temperature and pH.	16
Figure 8. Stain-free SDS-PAGE of ammonium sulfate precipitated protein	29
Figure 9. Zoomed in 0-0.5M NaCl gradient elution for IEX based purification of <i>T. fusca</i> crude enzymes	30
Figure 10. Zoomed in 0.5-2M NaCl gradient elution for IEX based purification of <i>T. fusca</i> crude enzymes	31
Figure 11. Coomassie stained SDS-PAGE of 0-0.5M NaCl IEX gradient elution	31
Figure 12. Coomassie stained SDS-PAGE of 0.5-2M NaCl IEX gradient elution.	32
Figure 13. SEC 650 Chromatography of IEX isolated Fraction II proteins	33
Figure 14. Coomassie stained SDS-PAGE of SEC 650 fractions and purified putative Cel6B in Lanes 2-3	33
Figure 15. Supernatant/pellet reducing sugars assay for HiTrap Q fraction on CI/CI.	35
Figure 16. CMC activity assay for HiTrao Q fraction	36
Figure 17. Coomassie stained SDS-PAGE for LC-MS	37
Figure 18. LC-MS result for the band at 102 kDa(Figure17) upper band	38
Figure 19. LC-MS result for the band at 65 kDa (Figure 17)	39
Figure 20. CI/CIII Crude enzyme assay DNS results	51
Figure 21. Crude enzyme pH dependence	52

Figure 22. Crude enzyme temperature dependence	52
Figure 23. Stain-free SDS-PAGE of CelE and CelE CBM3a reaction mixture supernatant	55
Figure 24. Stain-free SDS-PAGE of CelE and CelE-CBM3a reaction mixture washed pellet	56
Figure 25. DNS result for CI&CIII and CelE/CelE CBM3a hydrolysis assay.	57
Figure 26. Coomassie stained SDS-PAGE of CelE/CelE-CBM3a+CI/CIII assay pellet.	58
Figure 27. Synergism assay on CI/CIII	59

List of Tables

Table 1. Chromatographic steps employed during FPLC based purification	24
Table 2. Bradford assay and pNPC assay results of ammonium sulfate saturation experiments	28
Table 3. Microbradford assay for HiTrap Q fractions	34
Table 4. Spectral Counting Table	40
Table 5. Identified extracellular proteins of T.fusca grown on cellobiose.	44
Table 6. Crude enzyme activities on PASC, CI, and CIII for varying enzyme loadings and timepoints	51
Table 7. Purified Cel6B pH dependence assay	53
Table 8. CI/CIII assay with purified Cel6B alone	53

Chapter 1. Introduction

1.1 Research background

Lignocellulosic biomass (e.g., agricultural residues like corn stover, switchgrass, poplar) is a low-cost, abundant, sustainable and renewable feedstock source for making biofuels or bioproducts. It is composed primarily of cellulose (glucose polymer), lignin (aromatic polymers), and hemicellulose (mixed hexose/pentose polymer) that can be enzymatically deconstructed to fermentable soluble sugars like glucose and xylose. However, crystalline cellulose microfibrils are tightly embedded within plant cell walls and are inherently recalcitrant to enzymatic hydrolysis, which makes cost-effective conversion of biomass-to-biofuels a major challenge for biorefining operations. Pretreatment of biomass is therefore used as the first step in a cellulosic biorefinery to enhance the accessibility of sugar polymers embedded within the plant cell wall followed by enzymatic hydrolysis to convert cellulose to glucose. Pretreatments like ammonia fiber expansion (AFEX), steam explosion and dilute acid are commonly used prior to conducting enzymatic hydrolysis. A novel form of ammonia-based pretreatment, called extractive ammonia (EA), has been developed recently that is more effective than the AFEX process.¹ EA pretreatment has been shown to modify the crystalline structure of native cellulose-I allomorph (CI) to cellulose-III (CIII). The pretreatment causes a decrease in the intra-layer/intra-chain hydrogen bonds and increase in the inter-layer/inter-chain hydrogen bonds.² This change in cellulose allomorphic state has been reported to help improve the accessibility of fungal endocellulases.² It was observed that the increased synergistic activity was majorly due to improved endocellulase activity on cellulose-III as compared to cellulose-I.

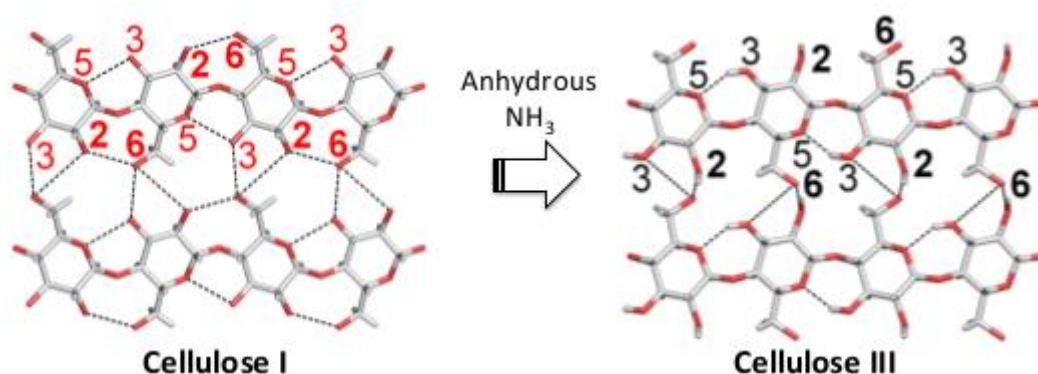


Figure 1. Impact of anhydrous liquid ammonia pretreatment on cellulose allomorphic structures. Top views of two truncated adjacent cellulose chains are shown for Cellulose-I and Cellulose-III crystalline fibril models. Dotted lines indicate intra-chain and inter-chain hydrogen bonding. Carbon atoms are numbered to locate relevant oxygen and hydrogen atoms involved in hydrogen bonding.

Figure adapted from Chundawat Shishir PS, Bellesia, Giovanni Uppugundla et al. Restructuring the Crystalline Cellulose Hydrogen Bond Network Enhances Its Depolymerization Rate, *J. Am. Chem. Soc.*, 133, 11163-11174 (2011).

Cellulases produced and secreted extracellularly by cellulolytic microorganisms *Trichoderma reesei* have been studied to optimize their activity on cellulose-III. The underlying mechanisms responsible for increased fungal cellulases hydrolysis rate have been explored in previous studies by Gao et al.³ The enhancement in apparent cellulase activity was attributed to the “amorphous-like” nature of the cellulose III fibril surface that facilitated easier single-cellulose chain extraction. Unrestricted substrate accessibility to active-site clefts of certain fungal endocellulase families was shown to further accelerate the enzymatic deconstruction of cellulose III. This result led to the hypothesis that enzyme cocktails isolated from other cellulolytic microorganisms like *Thermobifida fusca* that also secrete synergistic exo/endo-cellulases could also show a similar enhancement in activity towards cellulose-III.

Thermobifida fusca is a filamentous, thermophilic soil-based cellulolytic actinobacterium that grows at 50-55 °C and is reported to efficiently utilize cellulose as a carbon-source.⁴ *T. fusca* secretes a cocktail of six critical cellulase enzymes that

belong to glycosyl hydrolase (GH) families 5, 6, 9 and 48. The thermostability, broad pH range (pH 4 to 10), and high activity on cellulosic substrates have made cellulase enzymes produced by *T. fusca* a topic of increased research focuses again in recent years. Besides the thermal stability, another competitive advantage of *T. fusca* over most other cellulase expression systems is the fast growth rate and high temperature growth conditions that make it harder for the growth culture to get contaminated by other microbes. There have been several studies published on characterizing and isolating cellulases from crude enzyme mixtures produced by *T. fusca*.⁵ However, a detailed study characterizing the exocellulases, endocellulases and their synergistic activity on cellulose-I/III has not been reported previously. Among the seven enzymes directly purified or cloned from *T. fusca*, four of them are endocellulases (including Cel5A, Cel5B, Cel6A, and Cel9B), two of which are exocellulases (Cel6B and Cel48A), and one is a processive endocellulase (Cel9A) that is reported to have both endo-/exo-cellulase activities. During hydrolysis of microcrystalline cellulose, the cellulases in the cocktail are reported to work synergistically to break down cellulose. Endocellulases and exocellulases have distinct structural motifs that result in distinct affinity and catalytic activity due to subtle differences in cellulose structure. For example, endocellulases cleave the internal bonds of cellulose chains mostly and result in increasing reducing chain ends attached to the insoluble residual substrate. While exocellulases bind to and hydrolyze insoluble cellulose preferring the chain ends as initiation sites to mostly produce cellobiose. One popular mechanistic model explains endo-exo synergy as, endocellulases generating new reducing ends on the cellulose surface that serve as the initiation sites for exocellulases which might reveal additional endo-active sites, to eventually synergistically convert microcrystalline cellulose in to soluble sugars.⁶ Understanding of how major cellulolytic enzymes work and their

synergistic activity could help reduce the cost of enzymes needed for biofuels production and help make the cellulosic biorefineries commercially viable. After identification of suitable enzymes that synergize well together, we could further reduce enzyme usage by optimizing the ratio of enzymes necessary in the cocktail to maximize hydrolytic activity.

1.2 Aims of the project:

1. Measure the activity of soluble carboxymethylcellulose (CMC) grown *T. fusca* crude cellulase enzyme cocktail on crystalline cellulose-III.
2. Purification of exocellulase enzyme Cel6B from crude *T. fusca* secretomes and characterization of its activity under different conditions of temperature/pH.
3. Test the hypothesis that the enhanced overall activity of CIII stems from enhanced endo-activity for a bacterial cellulase system.

To achieve these three aims, the growth condition for *T. fusca* were optimized to maximize the crude enzymes' production, activities assayed on different cellulose allomorphs for the crude enzyme, and an enhanced hydrolytic activity on CIII was verified for *T. fusca* crude enzyme cocktail. Next, Cel6B exocellulase was purified using an optimized two steps purification, the purity was tested by SDS-PAGE and LC-MS/MS, and the activity of Cel6B were tested under different condition of temperature/pH on various substrate. Finally, synergistic endo-exo assays of Cel6B and CelE on CI/CIII were performed to test the endo-exo synergy hypothesis.

Chapter 2. Optimization of *T.fusca* growth conditions to maximize enzyme production

2.1 Materials and Methods

2.1.1 Cell culturing and sample preparation

The composition of Hagerdahl medium was similar to as described previously by Wilson D.B.⁷ For 500 mL culture medium preparation, 0.75 g NaCl (Thermo Scientific), 1.55 g (NH₄)₂SO₄ (Thermo Scientific), 4.55 g Na₂HPO₄ (Thermo Scientific), 0.45 g KH₂PO₄ (Thermo Scientific) and 485 mL DI water were added in to a 1000 mL conical flask to prepare the macro salts solution. The macro salts solution was then autoclaved and cooled down to room temperature. Alongside, a 300 mL 50X micro salts solution in DI water containing 0.75 g EDTA (Thermo Scientific), 0.3g MgSO₄.7H₂O (Acros Organics), 0.12 g ZnSO₄.7H₂O (Sigma Aldrich chemicals), 0.33g NH₄FeSO₄.6H₂O (Acros Organics), 0.214 g MnCl₂ (Acros Organics), and 0.396 g CaCl₂.2H₂O (Thermo Scientific) was prepared as well. Next, 5 mL of 2 g/mL cellobiose (Acros Organics), cEMD Millipore), glucose (Acros Organics) solution and 10 mL 50X micro salts solution were filter sterilized and added to the macro salts solution. The 50X micro salts solution was stored at 4°C. The macro salts solution and carbon source solutions were prepared freshly each time before use.

Original glycerol stock of *Thermobifida fusca* YX (kindly gifted by David Wilson's lab at Cornell University) was stored at -80 °C and 100 µL volume was inoculated in to 500 ml Hagerdahl medium containing different carbon sources (either 2% glucose (Sigma), 2% cellobiose (Sigma), or 2% CarboxyMethylCellulose or CMC (low viscosity carboxymethylcellulose sodium salt, Sigma) at desired pH (5.5, 6.5, or 7.5). Some

fermentations were conducted with 4% CMC. The pH of the medium was adjusted using 1M HCl or 1M NaOH. All substrate concentrations are in weight/volume basis (w/v). Growth culture was inoculated using a 50 mL pre-culture containing Hagerdahl medium and 2% glucose as carbon source. The pre-culture was centrifuged at 2000 rpm for 10 minutes, then the supernatant were discarded and the cell pellet were gently resuspended in 5 mL growth culture medium for inoculation. Briefly, three 50 mL precultures of *T. fusca* were grown at 50 °C and 200 rpm for 24 hours in a 300 mL Erlenmeyer flask in an orbital-shaking incubator (Innova Shaker, Eppendorf). Next, the bacterial cell pellet in the preculture were collected using a centrifuge, and the pellet was re-suspended in the 5 mL production culture medium and then inoculated in to 500 mL production culture medium. During the cell culture growth on various carbon sources, at predefined time points, 10 mL sample volumes were removed from the culture for secretomes characterization and activity analysis.

Pre-treatment of samples: Sample volumes removed from the culture were centrifuged (Centrifuge 5810 R, Eppendorf) at 10,000 rpm and 22 °C for 10 minutes to separate the cell pellet from the supernatant. The cell pellet was further analyzed for estimation of *T. fusca* growth rate.

Sonication: All subsequent procedures were conducted at 4 °C on ice. The cell pellet was transferred to 15 mL falcon centrifuge tubes, followed by addition of 5 mL 0.1M NaCl to wash the pellet. The mixture was next centrifuged at 4 °C, 1000 rpm for 10 minutes and the supernatants were finally discarded. Next, 1 mL working cell lysis buffer (composed of 20 mL 0.1 M phosphate buffer, pH 7, 10 mL 5M NaCl, 20 mL glycerol and 50mL deionized or DI water), 1 μ L lysozyme and 12.5 μ L protease

inhibitor cocktail (1 μ M E-64 Sigma Aldrich E3132, 0.5 mM Benzamidine and 1 mM EDTA) stock solution were added to the washed pellet, and then the mixtures were transferred in to a 2 mL microcentrifuge tube. The pellets were gently sonicated (Misonix Sonicator 3000, 1.6 mm diameter microtip) using an automated sonicator program set as follows: 3 seconds on and 30 seconds off for a total sonication time of 3 minutes on ice. The sonicated cell lysate mixtures were stored at -20 °C for further analysis.

2.1.2 Assays used for determination of protein concentration and activity of cellulases

All the assays in this thesis are performed in 96-well 0.3 mL flat-bottomed microplate (Greiner Bio-one) and 96-well round bottom microplate (Greiner Bio-one). Plates were sealed by adhesive based film covers to prevent evaporation losses (Greiner Bio-one). Bradford assays⁸ were used to measure the total protein concentration in the supernatant of the culture and the lysed cell mixtures of the cell pellet. The protein concentration of cytoplasmic proteins can be measured from the cell pellet lysate, which can be also normalized to the total number of *T. fusca* cells in the total culture volume. Cell lysis was achieved by sonication of the cell pellet as described above. The assays were done in 96 well microplates by adding 300 μ L Coomassie Plus (Pierce™ Coomassie Plus Bradford Assay Kit Thermo Scientific) Assay reagent, 10 μ L of unknown samples, blanks (buffer only) or BSA albumin standards ranging from 25 μ g/mL - 750 μ g/mL. The plates were gently shaken on a plate shaker for 30 seconds and incubated at room temperature for 10 minutes. Next, we measured the absorbance at 595 nm using a micro plate reader (Spectra Max Spectrophotometer, Molecular

Devices). The calibration curve plot of standards was obtained from standard wells. Using the slope of this plot, the protein concentration in the wells containing unknown samples was then calculated.

Model cellulose based small chromogenic mimic substrates such as p-nitrophenyl- β -D-cellobioside (pNPC) were used to measure the hydrolysis activity of the supernatant of *T. fusca* culture broth enriched in secreted cellulase enzymes. Before start, the broth was centrifuged using Centricon Plus-20 PLGC centrifuge filter unit (Millipore Sigma), 5mL broth were added to the filter tube and sealed with the cap, then centrifuged at 3000 rpm for 10 minutes. After 10 minutes the remaining volume were measured by pipette, for different samples the concentrate fold (original volume/concentrated volume) could be different from 1.5 to 2 folds, the protein concentrations were measured by Bradford assay and the final results of concentrations were multiplied by the concentrate folds. The time points broth samples were not concentrated, the temperature and pH optimization broths samples were concentrated used this method. Assays measuring the hydrolysis of 100 μ L of 2 mM 4-nitrophenyl β -D-cellobioside (Sigma Chemical Co.) dissolved in 50 mM pH 5 Na-acetate buffer as the substrate, along with 100 μ L concentrated (1.5-2 folds concentrated) *T. fusca* culture supernatant incubated at 50 °C for 4 hours. We stopped the reaction by adding 100 μ L 0.1 M NaOH and the well absorbances were read at 410 nm. The plot of standard curve was obtained from standard wells (i.e., pNP alone). Using the slope of the plot, the absorbances in the wells containing unknown samples can be converted to equivalent millimoles of pNP in each well. pNPC specific activity is defined as normalized total mM of pNP released by 1 mL original culture volume per mg protein (mM pNP/mL/mg) after 4 hours of pNPC hydrolysis.

2.1.3 Expression and purification of CelE and CelE-CBM3a

CelE/CelE-CBM3a pEC plasmids transformed *E. coli* BL21 glycerol stocks were used to inoculate LB liquid cultures to be grown overnight (stocks prepared by Chundawat and co-workers). For 500 ml LB medium, in 1 L shake flasks, the media was inoculated with 5% overnight grown cultures and grown at 37 °C until exponential phase. Protein expression was then induced using 0.5 mM IPTG at 37 °C for four hours. Cell pellets were collected by centrifuging the liquid cultures at 10,000 rpm for 15 minutes. Cell pellets were lysed using 15 ml cell lysis buffer (20 mM phosphate buffer, 500 mM NaCl, 20% (v/v) glycerol, pH 7.4), 200 μ l protease inhibitor cocktail (1 μ M E-64 from Sigma Aldrich E3132, 0.5 mM Benzamidine from Calbiochem 199001 and 1 mM EDTA from Fisher Scientific BP1201) and 15 μ l lysozyme (Sigma Aldrich) for every 3 g cell pellet. The cell lysis mixture was sonicated using Misonix sonicator 3000 at 4.5 output level and 10 seconds pulse-on time and 30 seconds pulse-off time for 5 minutes. The cell lysate was then centrifuged at 20,000 rpm, 4 °C for 45 minutes. Soluble cell lysate was then run on Nickel immobilized metal affinity column or IMAC column equilibrated in buffer A (100 mM MOPS, 500 mM NaCl, 10 mM Imidazole, pH 7.4) and eluted using buffer B (100 mM MOPS, 500 mM NaCl, 500 mM Imidazole, pH 7.4). Purified his-tagged proteins were desalted into 10 mM MES, pH 6.5 and purity characterized using SDS-PAGE.

2.2 Results

2.2.1 Screen of carbon source and growth time on cellulases expression

We first attempted to grow the bacterial culture by starting from the glycerol stock of *T. fusca* that was inoculated into LB medium and Hagerdahl medium. Both medium contained 0.2% (w/v) glucose as carbon source, however, after 72 hours there was no significant growth observed in the medium. Next, we tried a few different concentrations of the carbon source and found that higher carbon source loadings (e.g., 2%) gave significant culture growth (data not shown). While, Hagerdahl medium containing 2% glucose were found to give robust growth and therefore we decided to use Hagerdahl medium containing 2% (w/v) glucose to prepare starter cultures for all future experiments (unless stated otherwise). Next, the starter culture grown cell pellets was inoculated in to Hagerdahl medium containing different carbon sources (2% w/v). The protein concentration in the secretome broth (Figure 1) and the cell pellet (Figure 2) of the culture was determined at different fermentation time points.

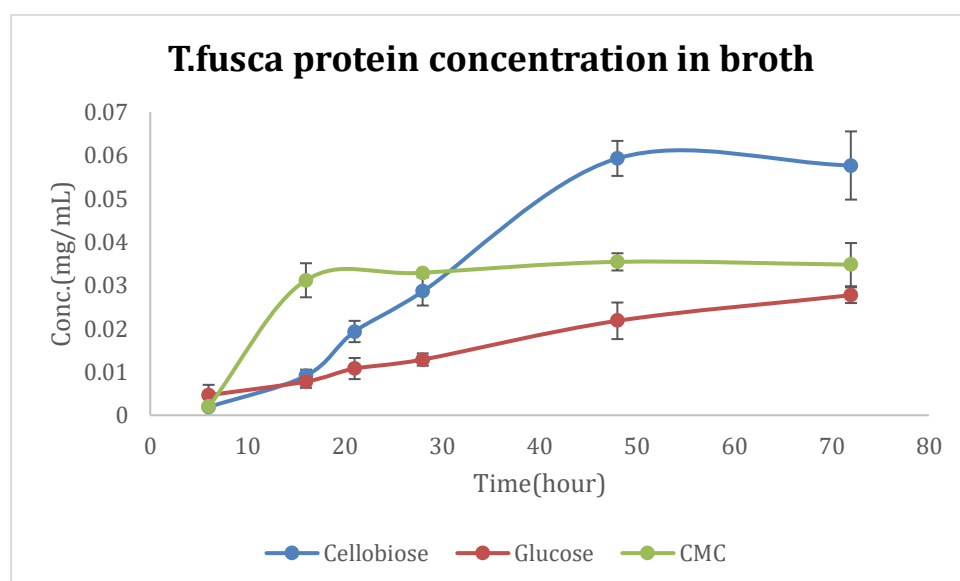


Figure 2. Protein concentration profile of fermentation broth of *T. fusca* grown on different carbon sources and at various growth time points.

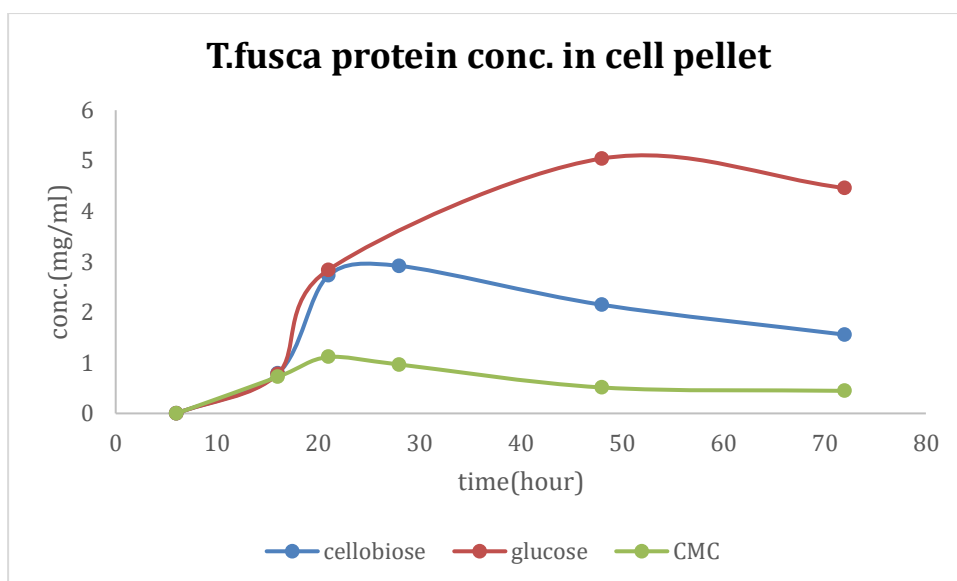


Figure 3. Protein concentration profile of fermentation cell pellets of *T. fusca* grown on different carbon sources and at various growth time points.

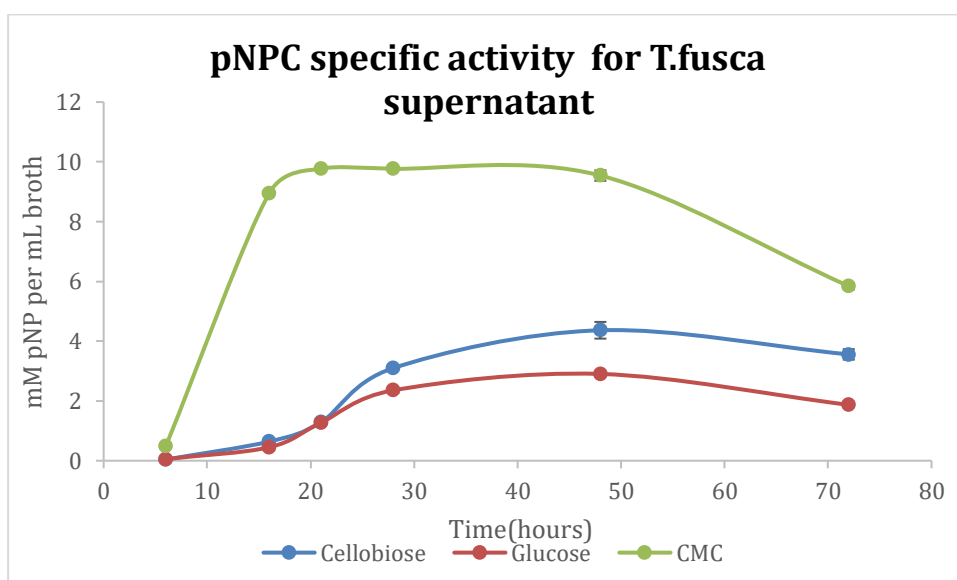


Figure 4. pNPC cellulase activity detected in *T. fusca* broth at various fermentation time points.

Note that pNPC activity is equal to mM pNP released after 4 hours of pNPC hydrolysis per mL of original broth volume.

Figure 4 shows the relative activity of cellulases expressed in the culture broth based on measured pNPC hydrolytic activity. The expressed cellulases had the highest activity for CMC carbon source at all the times compared to the cellulases expressed upon *T. fusca* growth on glucose or cellobiose. After 48 hours, the overall activity started to decrease, thus 48 hours was decided to be the optimal growth time for all future production cultures. Although the protein concentration of the pellet was low for

the CMC culture, the protein concentration detected in the fermentation broth was relatively not low. This suggests that the bacteria were able to rapidly express and secrete proteins/enzymes into the broth using CMC as a carbon source over other sources within the first 24 hours but were unable to grow to high cell densities. Since the carbon source concentrations were not normalized based on equivalent molar ratios of glucose or soluble sugars that would be available from each substrate, it is challenging to clearly resolve the underlying molecular mechanism responsible for more efficient protein expression seen with CMC. We speculate that chemical modifications of CMC (Note that degree of carboxymethyl substitution for low viscosity CMC should be close to 0.6) could also further reduce bioavailability of hydrolyzed sugars. This is clearly supported by the total cell culture growth rate as estimated from the total pellet protein concentration which is seen to be highest for glucose followed by cellobiose and finally followed by CMC at equi-mass starting concentrations. Since glucose is a lower molecular weight substrate than its dimer cellobiose (or CMC) the molar concentrations for glucose is highest in our experiments for an equi-mass loading starting concentration. This could explain why glucose resulted in the highest cell density growth over other carbon sources. But interestingly, using a more complex glucose polymer like CMC obviously resulted in producing more active cellulases for equivalent starting carbon source concentrations (based on an equivalent mass basis). We suspect that structurally more complex oligosaccharides released during CMC hydrolysis/modification by the basal cellulases expressed in the initial growth phase might trigger a stronger induction of the *T. fusca* cellulolytic expression machinery. One major advantage of using CMC over insoluble cellulosic biomass is that the recovery of bound cellulases from insoluble cellulose is poor due to irreversible binding to lignin/cellulose etc.⁹ CMC has been used as a carbon source for

other microbes to express cellulases such as *Archachatina marginata*¹⁰ and *Trichoderma viride*.¹¹

Besides, after 24 hours incubation of the growth culture, the viscosity of the culture were decreased significantly, which is an indication of most of the CMC was hydrolyzed/consumed by *T. fusca*. To maximize the growth, 4% (w/v) CMC was also used instead of 2% CMC. All broth samples were further analyzed via SDS-PAGE using stain free detection method to identify expressed proteins (BioRad, Stain-Free Gels). From Figure 5, we could see that the protein is most concentrated at 48 hours' time point for cellobiose (Lane3), while for CMC the different between 28 hours (Lane 4) and 48 hours (Lane 2) is not obvious. This result agrees with the Bradford assay result (Figure 2), where we found after 28 hours the growth rate was still increasing when we used cellobiose as carbon source. However, when we used CMC as carbon source the growth rate stopped increasing after 28 hours. Expected molecular weight of cellulases are: 65 kDa for Cel6B, 104 kDa for Cel48A, 50 kDa for Cel5A, 46 kDa for Cel6A, 101 kDa for Cel9B and 90 kDa for Cel9A. Extracellular proteins expression for *T. fusca* grown on cellobiose has been studied by the Wilson Lab.¹² For enzymes expressed when cells were grown on both cellobiose and CMC, there was a dominant band at 65 kDa, which was likely to be Cel6B. For enzymes grown on cellobiose, there was an abundant band at 54 kDa (with no clear band at 65 kDa), which could have been proteolyzed Cel6B or other enzymes. Cel6B was found to be the most abundant cellulase when the Wilson lab used cellobiose as carbon source. However, the molecular weight of expressed proteins detected in our study was lower than expected likely due to Cel6B proteolysis or due to differences in relative expression of other cellulases. Besides this, there was a low intensity band around 70 kDa, which could

have been Lam81A, a β -1,3-Glucanase according to Wilson's paper. Another band at 110 kDa appeared in enzymes produced from cells grown on cellobiose and CMC that could have been either Cel48A or Cel9B. From the SDS-PAGE analysis we could see that both cellobiose and CMC are likely good inducers for Cel6B expression. Cellobiose was seen to induce a greater variety of enzymes other than Cel6B (based on SDS-PAGE alone). But, the pNPC assay result suggested that CMC expressed enzymes had the highest activity over other carbon sources. Furthermore, since CMC is a new carbon source for *T. fusca* and has not been reported in the literature, we decided to use CMC as a carbon source to produce cellulases for large-scale expression and purification of Cel6B for this project.

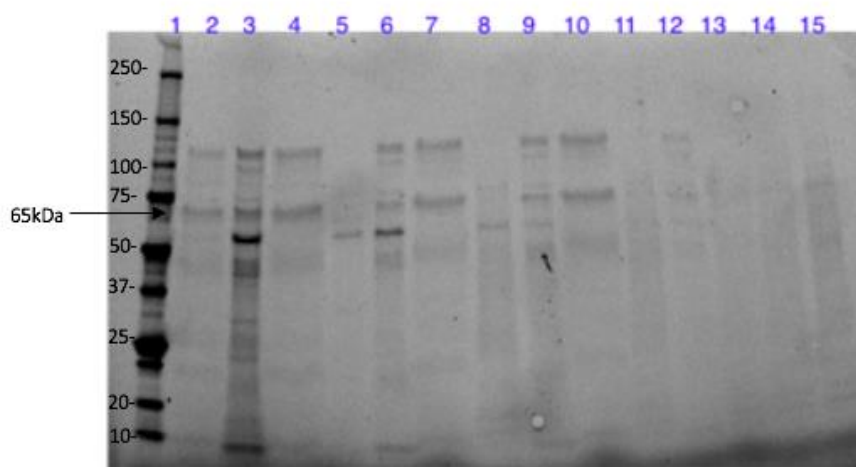


Figure 5. *T. fusca* culture broth secretomes highlighting expressed total proteins/enzymes for different carbon sources at various time points.

(From left to right, lane 1: standards; lane 2: CMC as carbon source at 48 hours; lane 3: Cellobiose as carbon source at 48 hours; lane 4: CMC as carbon source at 28 hours; lane 5: glucose as carbon source at 28 hours; lane 6: cellobiose as carbon source at 28 hours; lane 7: CMC as carbon source at 21 hours; lane 8: glucose as carbon source at 21 hours; lane 9: Cellobiose as carbon source at 21 hours; lane 10: CMC as carbon source at 16 hours; lane 11: Glucose as carbon source at 16 hours; lane 12: Cellobiose as carbon source at 16 hours; lane 13: CMC as carbon source at 6 hours; lane 14: Glucose as carbon source at 6 hours; lane 15: cellobiose as carbon source at 6 hours.)

2.2.2 Screen of growth temperature and pH

Growth curve and pNPC activity assays results indicated that bacterial growth and expressed cellulase enzyme activity were differentially impacted under various cell culture parameters. In order to further optimize the growth temperature and pH for the best performing carbon source, additional experiments were conducted. Using an equivalent volume of starter culture cell pellet suspension, fermentation was started using 4% CMC dissolved in sterile Hagerdahl medium in shake flasks at different starting pH's (5.5, 6.5 and 7.5) and shaken at 250 rpm. Next, we also incubated the cultures at 55°C and 60°C. After 48 hours, the protein concentrations of the concentrated culture broths were obtained using Bradford assays (Figure 5) and enzyme activities were determined using pNPC activity assays (Figure 6). In these experiments, there were noticeable differences in the gross morphology of *T. fusca* cells in the starter culture and production culture, cells grown in the starter culture aggregated into small puffballs, while the production culture forms cloudy-looking mixture. In previous study of *T. fusca* morphology by Deng and co-workers,¹³ they found that when cellobiose was used as carbon source cells grown in bioreactor aggregated into clumps while cells grown in shake flasks produced mycelia that connected cells in a web like fashion. The different morphologies were found to impact cellular growth significantly, as the dry cell weight of cells grown in the bioreactor decreased sharply after 10 hours compared to the cells grown in shake flasks. Also, the cells grown in shake flasks were found to express higher overall cellulase activity.¹³ Since *T. fusca* is a filamentous actinomycete, different stirring speeds and associated shear force regimes could easily impact the different cell morphologies seen during *T. fusca* growth. Also, since in these round of experiments we used 4% CMC solution that was significantly more viscous than the previous experiments conducted at 2% CMC, we hypothesize that the viscosity of the

solution due to varying initial CMC concentration in the production culture could impact the shear force experienced by cells. This could explain the differences in cell morphology and increased cellulase expression yields seen in these experiments.

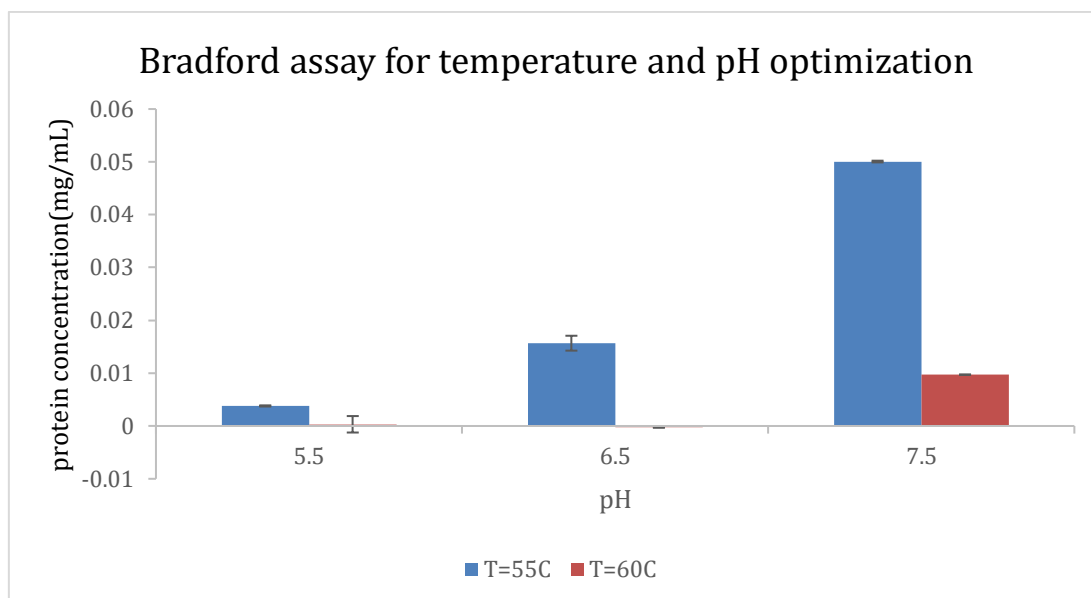


Figure 6. Bradford assay results *T. fusca* protein expressed in secretome broth at various temperatures and pHs.

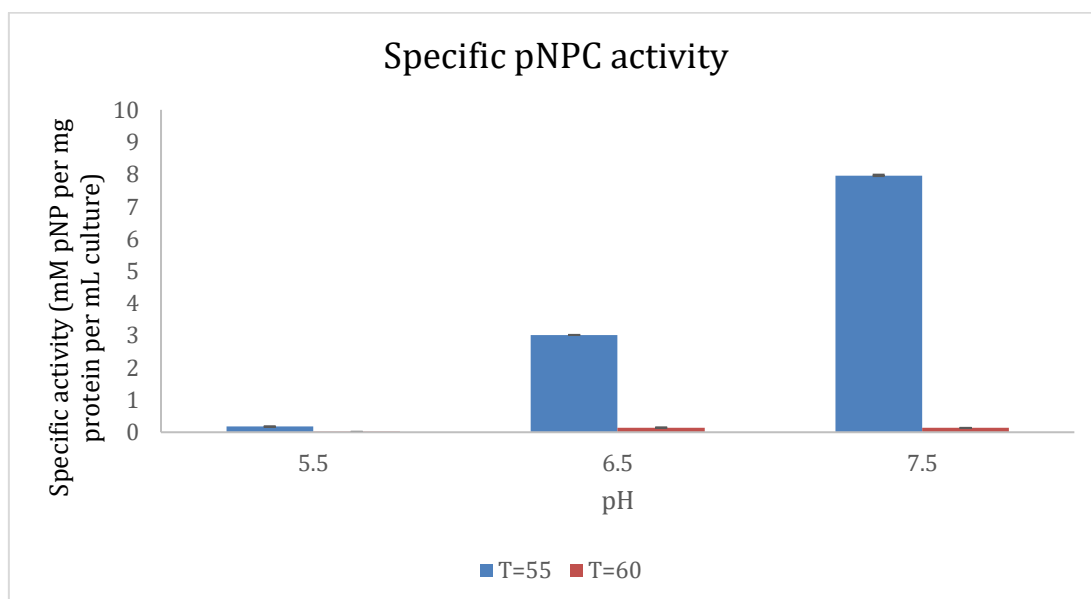


Figure 7. pNPC activity assay results of optimization of *T. fusca* culture growth temperature and pH.

As our results indicate, at pH 7.5 and 55°C the protein concentration in the broth reached 0.05 mg/mL, which is higher than all other culture conditions. Also, at pH 7.5 and 55°C, the expressed cellulases at 48 hours gave the highest pNPC activity.

2.3 Discussion

The *T. fusca* glycerol stock that were stored in the -80°C freezer were used initially as inoculums to prepare starter cultures. However, we found that the starter culture of *T. fusca* grew very slowly when directly inoculated from the original frozen stock, as there were not many cells seen growing in the start culture even after 24 hours. Improved cell growth was seen when we inoculated culture media using cell inoculums prepared from previous starter cultures and stored at 4°C.. When the previous starter culture was added (instead of growing cells directly from freezer stocks), the cells in the starter culture could grow into little puffballs instead of flocculent cells. Also, when we inoculated the puffball cells into the production culture, there was much better growth seen on the carbon source. One possible reason could be that the cells in glycerol stock were not viable enough to start growing immediately without a suitable lag time. Furthermore, the puffball morphology of the cells in the culture was also indicative of the viability of the cells to express cellulases. This further highlights the critical need to carefully prepare cellulolytic microbe cells cultures for maximizing cellulase expression yields. A similar phenomenon is commonly noted for other cellulolytic microbes like *T. reesei* that also need to be in an appropriate viable state, as also indicated by their filamentous fungal growth morphology, prior to initiating cellulase expression for large scale enzyme production.¹⁴

When preparing the culture medium, we also observed that the color of glucose turned brownish after directly autoclaving the media solution. Similar charring of sugars has been reported earlier and can result in modifying the underlying sugar chemical structure. Thus, to avoid structurally altering the carbon source, we used a 0.2 µm sterile

filter to sterilize the carbon source stock solutions after autoclaving the rest of the medium components separately. This method worked well for glucose and cellobiose, but CMC solution could not easily pass through the standard 0.2 μm filter due to the high viscosity of 2-4% CMC stock solutions. Even with a vacuum connection the filtration process was still very slow. It took more than 30 minutes to filter just 10 mL of stock CMC solution. Therefore, under this circumstance we set up another experiment to compare the difference between CMC based culture medium that was either autoclaved vs. filter sterilized. Fortunately, our cell culture results showed no significant difference between the performances of the two media on *T. fusca* growth or cellulase expression (data not shown). Next, we also used 4% (w/v) CMC for scaling-up cellulase production because this was the maximum solubility limit for our low-viscosity CMC substrate. However, when adding CMC directly in to DI water the dry solids always formed “clumps”, which were very hard to dissolve. The key step was to add the dry CMC solids carefully and slowly, so the solid could get well wetted and dissolve quickly. Sometimes even though there were some little clumps left in the culture it would be readily dissolved after the autoclave process.

Interestingly, we found that CMC was a much more effective carbon source (on an equi-mass loading basis) than cellobiose and glucose for inducing expression of cellulases. Furthermore, we found that 4% CMC carbon source based fermentation at pH 7.5 and 55°C for 48 hours allowed us to achieve maximum expressed protein/cellulase concentration in the secretome broth. After 48 hours fermentation, we saw a marked decrease of the solution viscosity that likely arises due to the hydrolysis of CMC by cellulases, as also seen previously in the literature during CMC based cellulase assays.⁵ Detailed characterization of the expressed cellulases and Cel6B

exocellulase enzyme isolation was next attempted using these optimized *T. fusca* cell culture conditions.

Chapter 3 Purification of Cel6B

3.1 Materials and methods

3.1.1 Ammonium sulfate saturation of the culture broth

Large-scale fermentation culture broth extracted by centrifugation of *T. fusca* cultures is a complex mixture of glycoside hydrolase enzymes that likely includes various cellulases, hemicellulases and/or certain auxiliary enzymes such as lytic polysaccharide monooxygenases (LPMOs) that are all encoded in the *T. fusca* bacterial genome. To ease up the process of purifying enzymes from such a complex secretomes broth on a laboratory scale using downstream techniques such as ion-exchange chromatography and gel filtration, it was essential to increase the concentration of enzymes in the mixture and reduce the total working volume of broth. Towards this end, ammonium sulfate mediated precipitation of the crude enzyme mixture was employed. Ammonium sulfate is a commonly employed inorganic salt that can be used to precipitate or ‘salt-out’ proteins at high concentrations. Various concentrations of ammonium sulfate were tested and the concentration that led to maximum concentration of protein and the maximum specific enzyme activity in the pelleted proteins, as estimated using Bradford and pNPC assays, was then used for further protein purification work. The figure/table later in this chapter highlights the specific pNPC activity of the precipitated crude cellulases mixture, as obtained for various ‘salting out’ concentrations of ammonium sulfate.

All protein precipitation steps were carried out at 0-4°C on ice. After 48 hours of growth, the *T. fusca* culture cell pellet and broth were separated by a high-speed centrifuge (Beckham Coulter Avanti J-E) at 14,000 rpm for 30 min. Next, the

centrifuged broth was filtered using a Buchner funnel and a vacuum line connected suction flask apparatus using filter paper (Whatman) to make sure no bacterial cell pellets were left in the broth. The volume of the broth was measured and 20% (w/v) ammonium sulfate was added slowly to the broth. After the ammonium sulfate dissolved into solution, the broth was allowed to sit on ice for 2-3 hours. Next, the precipitate and the remaining broth supernatant were separated by centrifugation as described previously. The protein-enriched precipitate was then re-dissolved in a small volume of 50 mM acetate buffer at pH 5. The remaining original cell culture broth volume was measured again, and a higher concentration of ammonium sulfate was added to the broth. The precipitation and the broth supernatant were separated and stored as detailed above. Similar steps were repeated for experiments conducted at 40%, 60%, 80%, and 100% (w/v) ammonium sulfate loadings.

3.1.2 Dialysis or desalting chromatography

After ammonium sulfate saturation based protein precipitation from the broth, the precipitate was dissolved in a suspension buffer. Desalting of the protein samples was needed, for residual salt removal, prior to further purification. Different methods such as dialysis and desalting cartridge columns were tested to assess the desalting efficiencies. In dialysis, the molecules in the solution would be separated based on their size through a semipermeable membrane; the dialysis bag membrane used had a nominal pore size and molecular weight cutoff for proteins of 10 kDa and smaller. The low molecular weight salts could thus be readily removed by diffusion driven by concentration difference across the membrane, while the large molecular weight proteins would be retained inside the dialysis bag. A sealed dialysis bag with redissolved protein sample was placed in a container that has 100x volume of 4°C

chilled target buffer, which was 20 mM Tris-HCl at pH 8 in our case. After every 12 hours, the buffer in the container was replaced. After 36 hours, the dialysis was completed and the protein in the dialysis bag could be recovered and flash frozen for short-term or longer-term storage at -20 or -80°C, respectively. An alternative to dialysis for salt removal was the use of pre-packed desalting/buffer exchange columns using the standard NGC FPLC system available in our laboratory (Bio-Rad).

3.1.3 Ion-Exchange (IEX) chromatography

Enzyme purification/polishing was performed using the NGC FPLC system (Bio-Rad) after filtering all protein samples using a 0.2 µm filter (EMD Millipore). Milli-Q based DI water was used to prepare all buffers and 5M HCl (SPEX CertiPrep) was used to adjust the pH of Tris-base buffer (Sigma-Aldrich). Buffers were all filtered through 0.2 µm using Vacuum Filtration Bottle (Argos Technologies) and degassed prior to use on the FPLC.

The crude enzyme contains a complex mixture of proteins that have different isoelectric points (pI) ranging from 4.0 to 7.5 based on previously published results, with Cel6B reported to have a pI of 4.1.¹² To remove all other undesired *T. fusca* proteins from Cel6B, ion-exchange chromatography (IEX) was used as the first step for protein purification prior to additional polishing steps using other chromatography methods. Using a 5 ml HiTrap Q (GE Healthcare) anion-exchange column, different buffer pHs ranging from 6 to 8 were tested, with pH 8 giving the best separation between *T. fusca*'s acidic pI cellulases. When the pH of the buffer is greater than the pI of the protein, the protein would be negatively charged and would therefore bind tightly to the anion-exchange column allowing better separation efficiency upon elution from the column

at increasing salt concentrations. The crude protein was therefore desalted into 20 mM pH 8 Tris-HCl buffer 'A' and loaded on to the equilibrated column at a flow rate of 0.5 mL/min. Next, 20 mM Tris-HCl buffer at pH 8 containing 0.5 M NaCl (Thermo Scientific) was used as the elution buffer 'B' in combination with the loading buffer. After 0-0.5 M gradient elution was completed, the buffer B was changed to 20 mM pH 8 Tris-HCl buffer containing 2 M NaCl instead and a new round of gradient elution were started. The sequential IEX purification steps are highlighted in Table 1 later in this chapter. An increasing elution buffer gradient was then started, that allowed proteins of varying acidic pI's to be eluted from the column at higher salt concentrations. The eluted protein fractions were collected using the NGC fraction collector, analyzed for purity via SDS-PAGE, and activity characterized using model substrate hydrolysis assays (as described later).

3.1.4 Size Exclusion chromatography

To further polish and purify the isolated Cel6B enzyme, size exclusion columns (SEC) Enrich SEC 650 (Bio-rad) was used as a secondary polishing step. The size exclusion columns were prepacked with porous spherical polymer resin beads, which allow separation of proteins based on differences in their molecular weights. Appropriate aliquot volumes (0.75 mL) of peak 5 collected from IEX, enriched in Cel6B, were loaded on to a SEC column pre-equilibrated with 20 mM pH 7 Tris-HCl buffer and containing 100 mM NaCl (Thermo Scientific) at a flow rate of 0.5 mL/min. The SEC elution peaks, after running the mobile phase for one column volume (CV), were collected and analyzed for purity by SDS-PAGE and activity characterized using model substrate hydrolysis assays.

Step	Sample type	Column and buffer	Gradient/Mobile Phase	Flowrate (mL/min)
1.1	Buffer exchanged re-dissolved crude broth enzymes	5 mL HiTrap Q A: 20 mM Tris HCl pH8 B: A+0.5 M NaCl	2 mL sample 10 CV, 0-100% B	0.5
1.2	Remaining bound protein on the column after step 1.1	5 mL HiTrap Q A: 20mM Tris HCl pH8 B: A+2M NaCl	20 CV, 0-65% B	1
2.0	Peak 5 eluting from column in 1.2	5 mL HiTrap desalting A: 20 mM Tris HCl pH7 + 100 mM NaCl	1.5 mL sample 1CV, 100% A	5
3.0	Major peak isolated from 2.0	24 mL SEC650 A: 20 mM Tris HCl pH7 + 100 mM NaCl	0.75 mL sample 1CV, 100% A	0.5

Table 1. Chromatographic steps employed during FPLC purification of Cel6B from *T. fusca* crude secretome

3.1.5 Activity assays for eluted FPLC protein fractions

Microbradford assay was used to estimate the protein concentration of all collected fractions (in addition to monitoring protein concentration using UV 280 nm absorbance detector on the FPLC). Briefly, 150 μ L of Bradford reagent and 150 μ L of fractions were added in to a 96-well flat bottom microplate, incubated at room temperature for 10 minutes and then well absorbances were measured at 595 nm. The background noise was subtracted out using suitable buffer blanks, and the protein concentrations estimated via a calibration curve using BSA as standards.

CMC was used as substrate to estimate the overall cellulase activity of all the collected FPLC fractions. Briefly, 60 μ L of collected fractions were directly added in to a 96-well microplate containing 40 μ L of 10 g/L CMC solution and incubated at 55 °C for 24 hours. After 24 hours, 30 μ L of the supernatant was taken for analysis of released total reducing sugar using the standard dinitrosalicylic acid or DNS assay.¹⁵ Microcrystalline Avicel based cellulose-I (CI) was used to prepare cellulose-III (CIII) as described previously by Chundawat et al.² CIII was kindly prepared by Dr. Leonardo Sousa at MSU (East Lansing, MI). Enzymatic hydrolysis assays were conducted on CI and CIII directly using the eluted protein fractions. However, instead of only

monitoring the released soluble sugars in the supernatant, the total reducing ends associated with the insoluble cellulose pellet was also estimated. The reducing sugar content measured in the supernatant and pellet was used to approximately estimate the associated endocellulase and exocellulase activities in the eluted FPLC fractions, respectively.¹⁶ Based on our current mechanistic models of how non-complexed cellulases from *T. reesei* or *T. fusca* act on cellulose, exocellulases are expected to hydrolyze insoluble cellulose chain ends to produce soluble cellobiose, while endocellulases are expected to mostly make random cuts in middle of cellulose chains leaving reducing chain ends associated with the residual insoluble substrate. Thus, by determining the effective reducing sugar concentration distribution between the insoluble pellet and the supernatant after hydrolysis allows one to approximately calculate the relative exocellulases vs. endocellulases activities. Briefly, 40 μ L of 10 g/L CI or CIII stock solutions were added to 60 μ L collected FPLC fractions in a 96-well round bottom microplate, and incubated for 24 hours at 55 °C with 5 rpm end-over-end mixing. At the end of 24 hrs, the plates were centrifuged at 2000 rpm for 5 min and 30 μ L supernatant was taken for DNS assay. While, the remaining supernatant was carefully removed by a pipette, and the insoluble cellulose pellets were washed extensively four times with 200 μ L of 20 mM pH 8 Tris-HCl buffer (identical to column elution buffer). After washing the pellet, it was resuspended in 60 μ L Tris-HCl buffer to re-adjust the final volume back to 100 μ L. The concentrations of reducing sugars in the original hydrolysate supernatant and the washed cellulose pellet were then estimated using standard DNS assay methods.

3.1.6 LC-MS identification of proteins from SDS-PAGE

Protein bands from Coomassie stained SDS-PAGE gel were cut out into small rectangular pieces (2x1 mm). In gel digestion and proteomics analysis using liquid chromatography tandem mass spectrometry (LC-MS/MS) was then performed by Ms. Amenah Soherwardy at the biological mass spectrometry proteomics facility at Rutgers University (New Brunswick). Each gel band was subjected to reduction with 10 mM DTT for 30 min at 60°C, followed by alkylation with 20 mM iodoacetamide for 45min at room temperature in the dark and finally digestion with sequencing grade trypsin (Thermo Scientific Cat#90058) by incubation overnight at 37°C. Peptides were extracted twice with 5% formic acid, 60% acetonitrile, and then dried under vacuum. Next, the peptides were solubilized in 12.5 µl 0.1% trifluoroacetic acid aqueous solution, and analyzed by Nano LC-MS/MS (Dionex Ultimate 3000 RLSCnano System interfaced with a QExactive HF from ThermoFisher). Briefly, 1µl of each sample was loaded onto a self-packed 100 µm x 2 cm trap (Magic C18AQ, 5µm 200 Å, Michrom Bioresources, Inc.) and washed with Buffer A (0.2% formic acid) for 5 min with a mobile phase flow rate of 10 µl/min. The trap was brought in-line with the analytical column (Magic C18AQ, 3 µm 200 Å, 75 µm x 50 cm) and peptides fractionated at 300 nL/min using a segmented linear gradient of 4-15% B (0.2% formic acid in acetonitrile) for 5min, 15-50% B for 50min, 50-90% B for 5 min and finally held at 90% B for 5 min. Mass spectrometry data was acquired using a data-dependent acquisition procedure with a cyclic series of a full scan acquired with resolution of 120,000 followed by MS/MS (HCD with relative collision energy of 27% and resolution of 30,000) of the 20 most intense ions and a dynamic exclusion duration of 20 sec. The detected mass to charge (m/z) peaks list of the LC-MS/MS was generated from raw file by Thermo Proteomoe Discoverer (v. 2.1) as mgf format and searched against the

Thermobifida fusca (NC_007333) database, custom sequences (Q60029_THEFU Glucanase and Q47NH7_THEFY Cellulose 1,4-beta-cellobiosidase OS=*Thermobifida fusca*) and a database composed of common lab contaminants using an in house version of X!Tandem (GPM Furry, Craig and Beavis, 2004). Search parameters were as follows: fragment mass error: 20 ppm, parent mass error: +/- 7 ppm; fixed modification: carbamidomethylation on cysteine; flexible modifications: Oxidation on Methionine, acetylation at the protein N-terminus. For refine oxidation and dioxidation of tryptophan, dioxidation of methionine, as well as deamidation of Asparagine and Glutamine were also considered as potential modifications. Protease specificity was trypsin (C-terminal of R/K unless followed by P) with 1 miss-cut at preliminary search and 5 miss-cut during refinement. Only spectra with top hit of $\log e < -2$ were included in the final tabulated spectral counts report.

3.2 Results

3.2.1 Optimization of ammonium sulfate saturation concentration

The amount of total precipitate obtained from the *T. fusca* fermentation broth was visually seen to increase from 20% to 60% (w/v) ammonium sulfate loadings. However, at 60% ammonium sulfate loading and higher, the viscosity of the precipitate became very high and the precipitate could not be fully dissolved back into the re-solubilization buffer. We suspect this indicated the high concentrations of residual CMC from the broth was also precipitating out of solution along with the proteins at higher ammonium sulfate concentrations. Since the CMC cannot be removed by dialysis and because the residual CMC in the enzyme sample could interfere during enzymatic assays, we had to ensure no CMC was being recovered along with the precipitated crude enzymes. The specific pNPC activities for precipitates recovered from various ammonium-loading

experiments were used to also deduce the optimal salt concentration loading. Details on the Bradford and pNPC activity assays for all cases are reported in table 2 below. The original supernatant from the cell culture for these experiments was too dilute and not in the assay range.

Ammonium sulfate (% , w/v)	C ₀ -protein concentration (mg/mL)	A ₀ -mM pNP released in the well (mM)	A ₁ -mM pNP per mL culture	A ₂ -specific activity (mM/total protein amount)
0% original	n.d.	n.d.	n.d.	n.d.
20%	0.04	0.35	10.36	86.00
40%	0.59	31.51	1575.70	530.63
60%	0.08	0.44	66.41	54.61

Table 2. Bradford protein assay and pNPC activity assay results of ammonium sulfate saturation experiments

**n.d. means either not detected or value too small to be detected by the current assay*

At and beyond 60% (w/v), the concentration reached the maximum solubility of ammonium sulfate, which led to a lot of undissolved ammonium sulfate being precipitated along with the protein as well. In our experiments, 40% ammonium sulfate was found to be optimal, which is also similar to results from previous work.⁷ The precipitates formed using 40% ammonium sulfate concentration were next re-dissolved in suitable buffer, dialyzed, and run on SDS-PAGE gel (Figure 8).

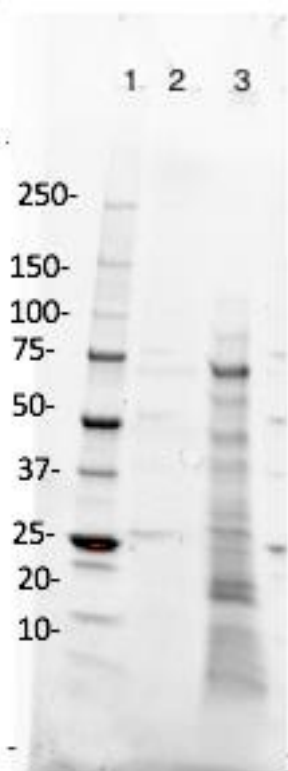


Figure 8. Stain-free SDS-PAGE of ammonium sulfate precipitated protein

Here, Lane 1: marker; Lane 2: empty; Lane 3: dialyzed 40% ammonium sulfate precipitation sample.

3.2.2 Ion-Exchange chromatography purification of Cel6B and other cellulases

Next, 2 mL of desalted crude enzyme recovered after 40% loading ammonium sulfate precipitation was loaded on to an equilibrated IEX column at a flow rate of 0.5 mL/min, and the bound proteins then eluted with 50 mL gradient from 0 to 0.5 M NaCl enriched 20 mM Tris-HCl buffer (pH 8). Upon gradient elution at increasing salt concentrations, three protein peaks (named as peak 1, peak 2, and peak 3) detected using the UV 280 nm detector (Figure 9) were collected and analyzed via SDS-PAGE. Next, the second round of sequential gradient elution from 0.5 M to 2 M NaCl enriched in 20 mM Tris-HCl (pH 8) was started at a flow rate of 2 mL/min for 100 minutes which resulted additional protein peaks (named peak 4, peak 5, and peak 6) that were collected for analysis. The protein fractions were run on pre-cast stain free SDS-PAGE gels (BioRad) at 200 V for 40 minutes and analyzed in the BioRad Gel Doc Imager using both

Stain Free and Coomassie blue staining based protein detection methods. Peak 1 was found to give mostly detected protein band at 17 kDa and a very low intensity band at 44 kDa (Figure 11). Peak 2 gave two protein bands, with one of the more intense bands around 35 kDa (see Lanes 5-6 in Figure 11). Peak 3 fractions gave multiple protein bands ranging between 50-90 kDa (see Lanes 10-15 in Figure 11). For peak 4, there was an intense band at around 62 kDa, which was very close to the molecular weight expected for our target protein Cel6B (~60 kDa). To get a better separation for proteins in this elution volume targeting Cel6B, a lower flow rate at 1.0 mL/min was used (Figure 10). Here we named the eluting fractions from the deconvoluted peak 4 that contained one protein band around 62 kDa as Fraction I, while the eluting fractions from peak 5 that contained 2 bands around 102 kDa and 62 kDa were named as Fraction II. All protein fractions were flash frozen with liquid nitrogen then stored at -80°C for long-term storage and further analysis.

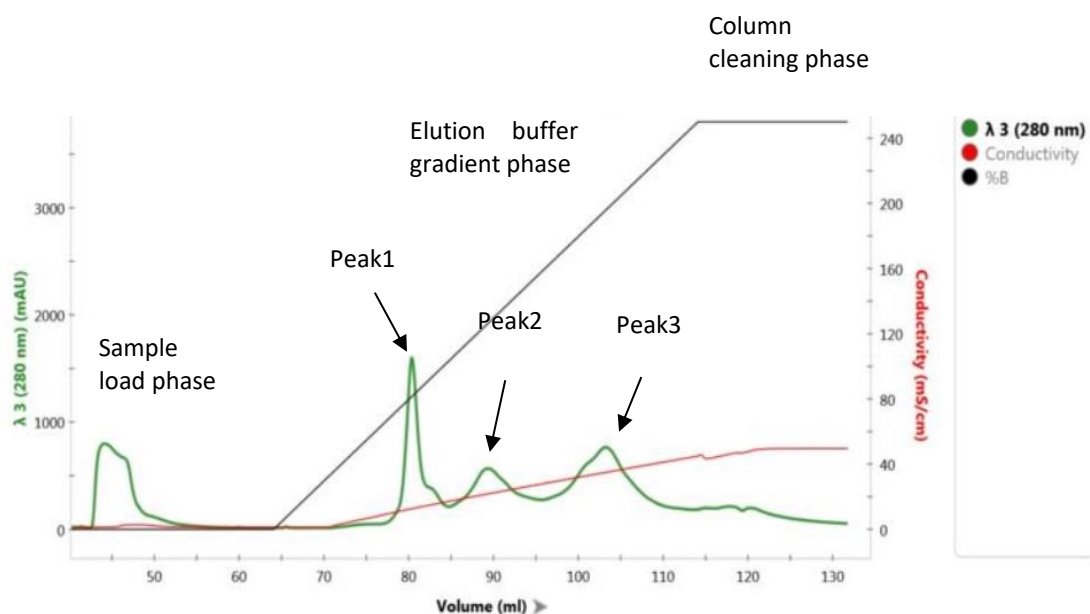


Figure 9. Zoomed in 0-0.5 M NaCl gradient elution for IEX based purification of *T. fusca* crude enzymes

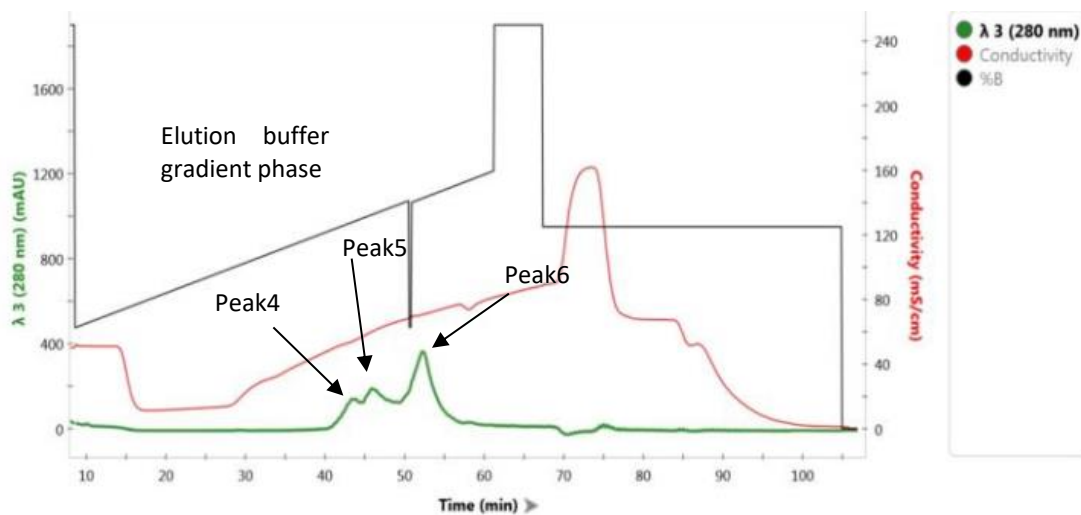


Figure 10. Zoomed in 0.5-2 M NaCl gradient elution for IEX based purification of *T. fusca* crude enzymes

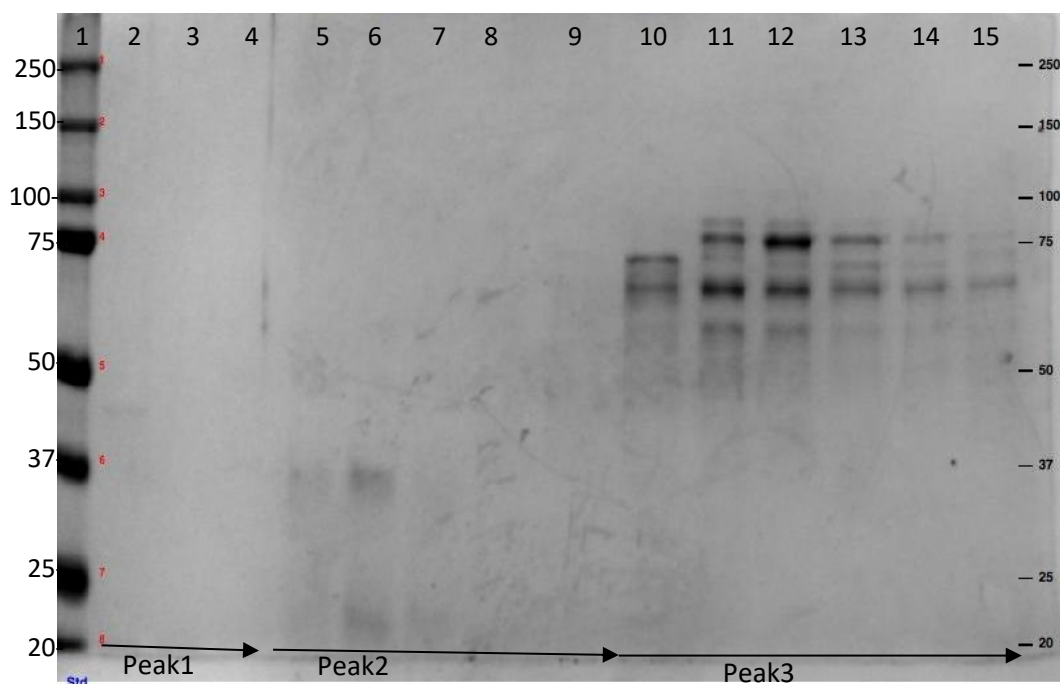


Figure 11. Coomassie stained SDS-PAGE of 0-0.5M NaCl IEX gradient elution

Here, Lane 1: protein marker; Lane2, 3: Peak 1 fractions; Lane 4-8: Peak 2; Lane 10-15: Peak 3.

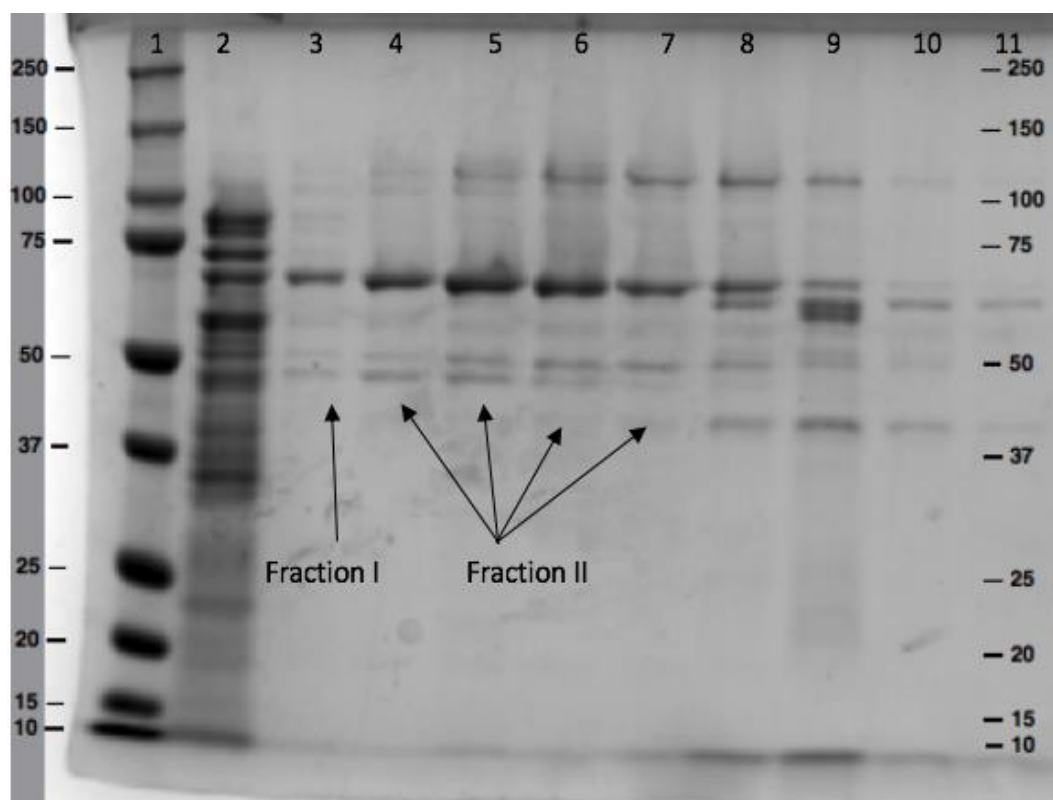


Figure 12. Coomassie stained SDS-PAGE of 0.5-2 M NaCl IEX gradient elution

Here, Lane2 is the mixture of proteins eluted from 0-0.5 M gradient elution.

3.2.3 Size exclusion chromatography polishing of Cel6B

Next, 0.75 mL of pooled Fraction II (see lanes 4-6 in Figure 12) was loaded onto a SEC 650 column (Bio-Rad), with the eluting 7 mL fractions that were collected and analyzed via SDS-PAGE. From the SDS-PAGE results, we noted that we got marginal separation between the 62 and 102 kDa proteins. It is likely that there is some inter-protein interactions between these cellulases in their native state that make it challenging to fully separate them based on size exclusion alone. Nevertheless, we were still able to separate some putative Cel6B protein (close to electrophoretic homogeneity) in the earlier eluting first two fractions (see lanes 2 and 3 in Figure 14).

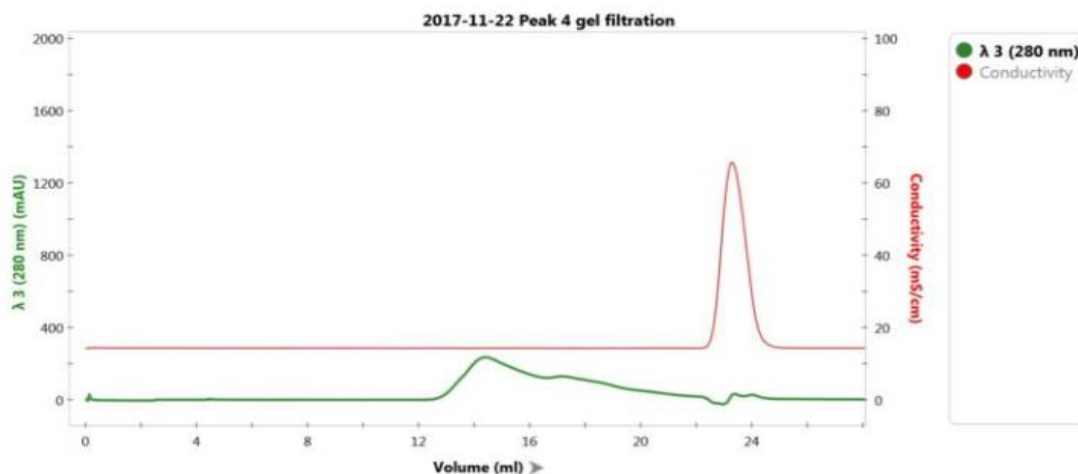


Figure 13. SEC 650 Chromatography of IEX isolated Fraction II proteins

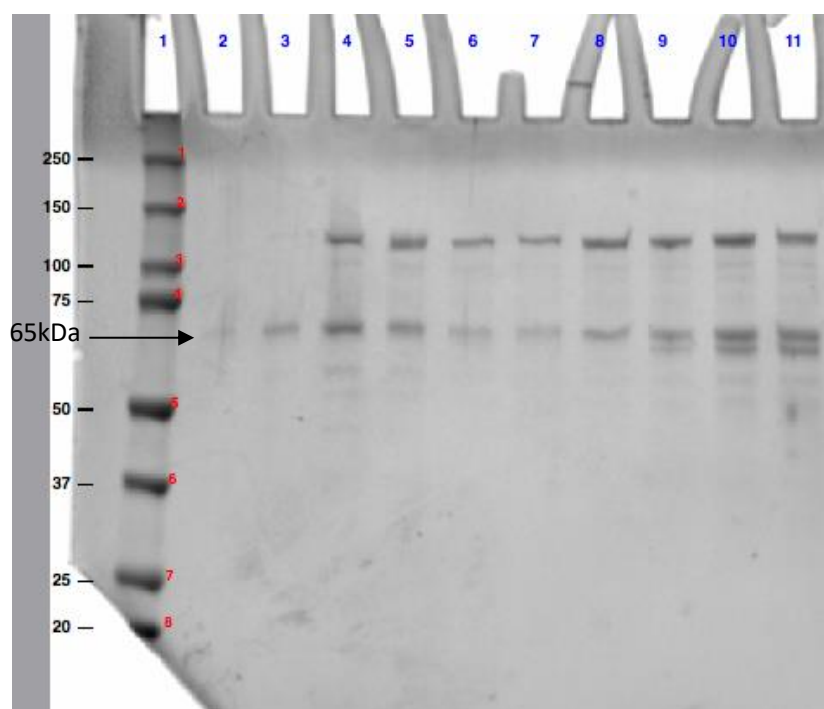


Figure 14. Coomassie stained SDS-PAGE of SEC 650 fractions and purified putative Cel6B in Lanes 2-3

3.2.4 Activity assay results

1. MicroBradford assay for IEX protein fractions

Eluting protein fractions from peaks 1-3, from the Hitrap Q IEX column (Figure 11), were analyzed for protein concentration using the MicroBradford assay. See summarized results in table below.

FRACTION	LANE 3	LANE 6	LANE10	LANE 11	LANE 12	LANE 13
PROTEIN CONC.(UG/ML)	21.18	23.97	16.33	31.74	37.52	40.87
STANDARD ERROR	0.73	0.18	0.13	1.09	0.27	0.35

Table 3. Microbradford assay for HiTrap Q eluting protein fractions

2. Cellulose allomorphs (CI/CIII) hydrolysis activity assay for supernatant vs. insoluble pellet

Enzymatic hydrolysis activity for IEX eluent fractions collected from HiTrap Q column, namely peaks 1-3 was characterized next on CI and CIII. We were interested in testing the relative exo-cellulase vs. endo-cellulase activity of the corresponding protein fractions by measuring the total reducing sugars detected in the supernatant vs. the insoluble cellulose pellet, respectively. Lane 3 corresponds to a fraction collected from peak 1, lane 6 corresponds to a fraction collected from peak 2, and lanes 10-13 correspond to fractions collected from peak 3. All corresponding lanes are depicted in the SDS-PAGE Figure 11. In the supernatant, the substrate blank wells (i.e., with no enzyme added) and the protein blank wells (i.e., no cellulose added) gave no reducing sugar readings. Peak 1 (lane 3 bands) did not show any released soluble sugars in the supernatant, although there were low-intensity protein bands seen on the SDS-PAGE. We suspect these bands correspond to non-cellulolytic enzymes like xylanases etc. For peak 2, the supernatant gave a very low reducing sugar concentration for CI at 0.0016 mg/mL, while the same protein fraction gave 0.0138 mg/mL for CIII, which indicates that the proteins eluting within peak 2 had a much higher relative activity on CIII compared to CI. There was an increasing trend of reducing sugar concentrations in protein fractions from peak 3, with lane 13 reaching a maximum sugar concentration at 0.0974 mg/mL for CI versus 0.1033 mg/mL for CIII. However, the difference between soluble sugars released from CI and CIII is marginal and not significant for most protein

fractions. But interestingly, based on the pellet assay, peak 1 and peak 2 mostly showed slightly higher reducing end concentrations than the substrate blank for CI/CIII, while peak 3 fractions were around the same as the substrate blank for both CI and CIII.

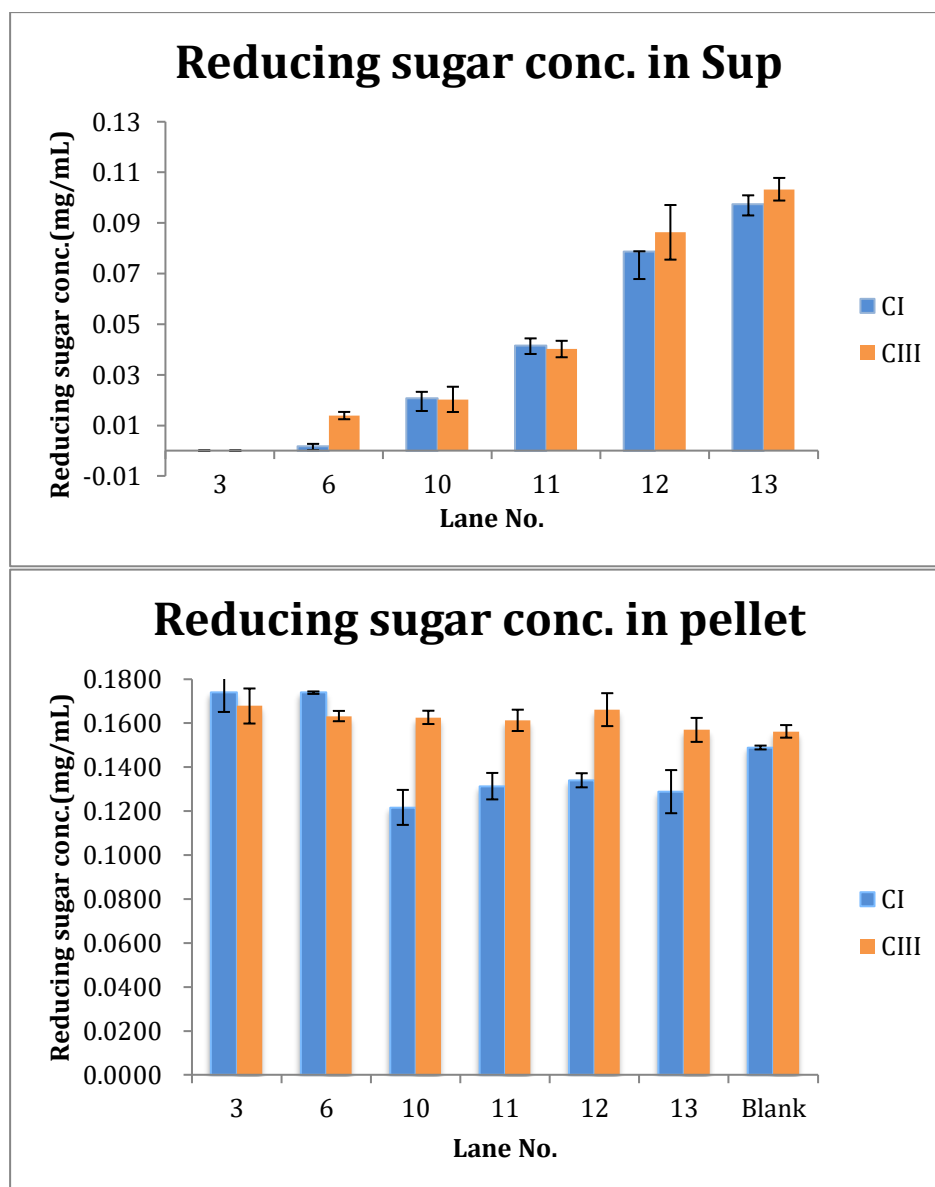


Figure 15. Supernatant versus cellulose pellet reducing sugars assay for HiTrap Q fraction on CI/CIII.

Top: supernatant reducing sugar concentration; Bottom: insoluble cellulose pellet reducing sugar concentrations.

3. CMCase activity assay

CMC is a soluble modified cellulose substrate, and cellulase activity on this substrate

is often representative of endoglucanase activity.¹⁸ Peak 1 (lane 3 bands) did show significant activity on CMC compared to other fractions from peak 2 and peak 3. Surprisingly, peak 2 (lane 6 bands) did not show intense bands on the SDS-PAGE but had a very high reducing sugar concentration released for CMC, almost the same or even higher compared to fractions from peak 3. The high activity on CMC for peak 3 agreed with the bands we have seen on SDS-PAGE (figure 11), as the protein fractions are likely enriched in a mixture of endocellulases and exocellulases.

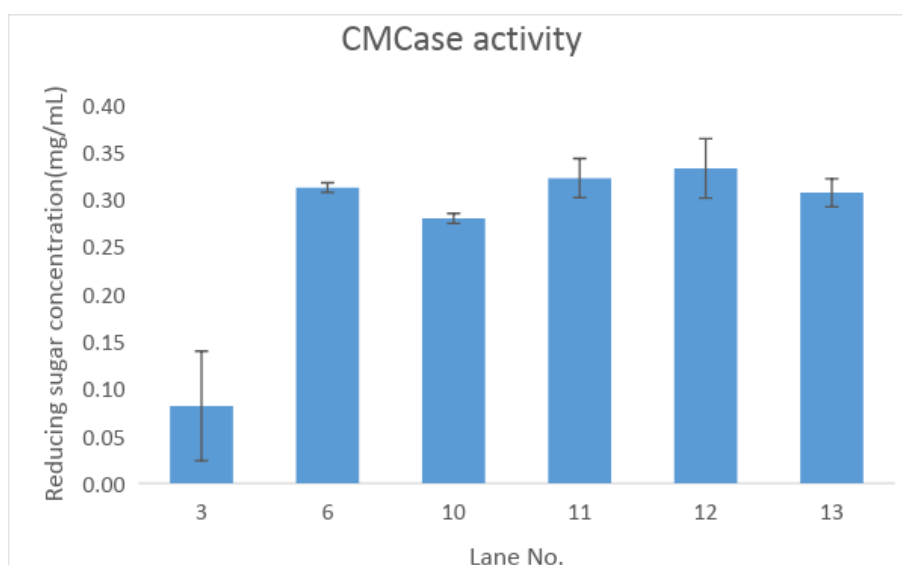


Figure 16. CMC activity assay for HiTrao Q fraction

3.2.5 LC-MS/MS proteomics analysis to validate Cel6B and other cellulase fractions

Next, in order to validate the identity of the eluted ~65 and ~102 kDa proteins, we used proteomics sequencing after standard trypsin digestion. Briefly, 10 μ L of Fraction I (figure 12) and fraction II (figure 12) eluted from HiTrap Q were loaded onto a new SDS-PAGE gel (Biorad precast gel TGX mini protein). Each protein band corresponded to 0.5 μ g protein as confirmed by Bradford assay. Bands highlighted using red circles in the gel image were cut out and send for LC-MS based proteomics analysis. From the proteomics result, the upper band around 102 kDa (which we assumed to be Cel48A) had indeed turned out to be a mixture of Cel48A and GH9

protein (gi|72162028|). While the lower band around 65 kDa was confirmed to be Cel6B alone with no other coeluting *T. fusca* proteins detected.

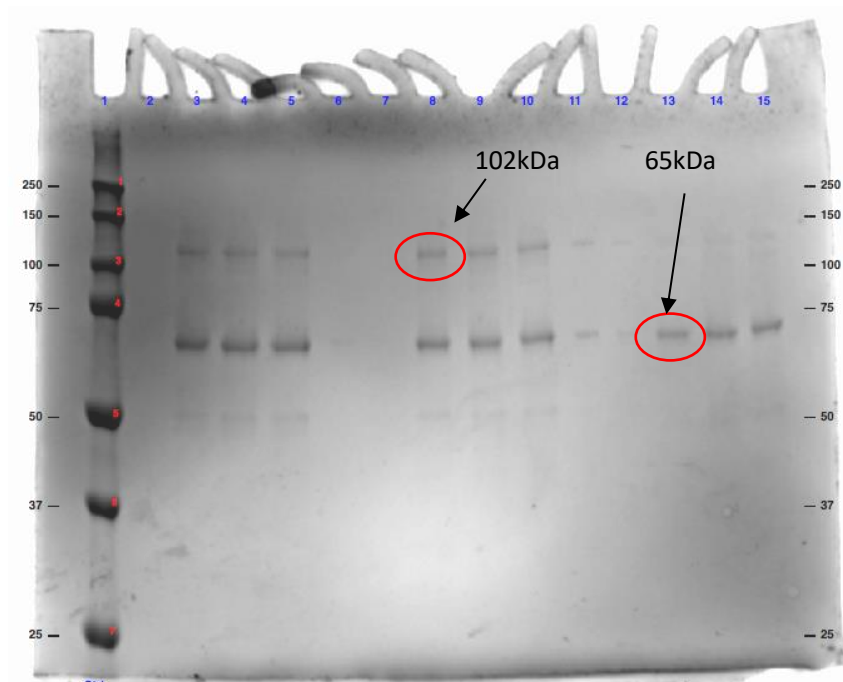


Figure 17. Coomassie stained SDS-PAGE highlighting protein bands cutout for LC-MS analysis

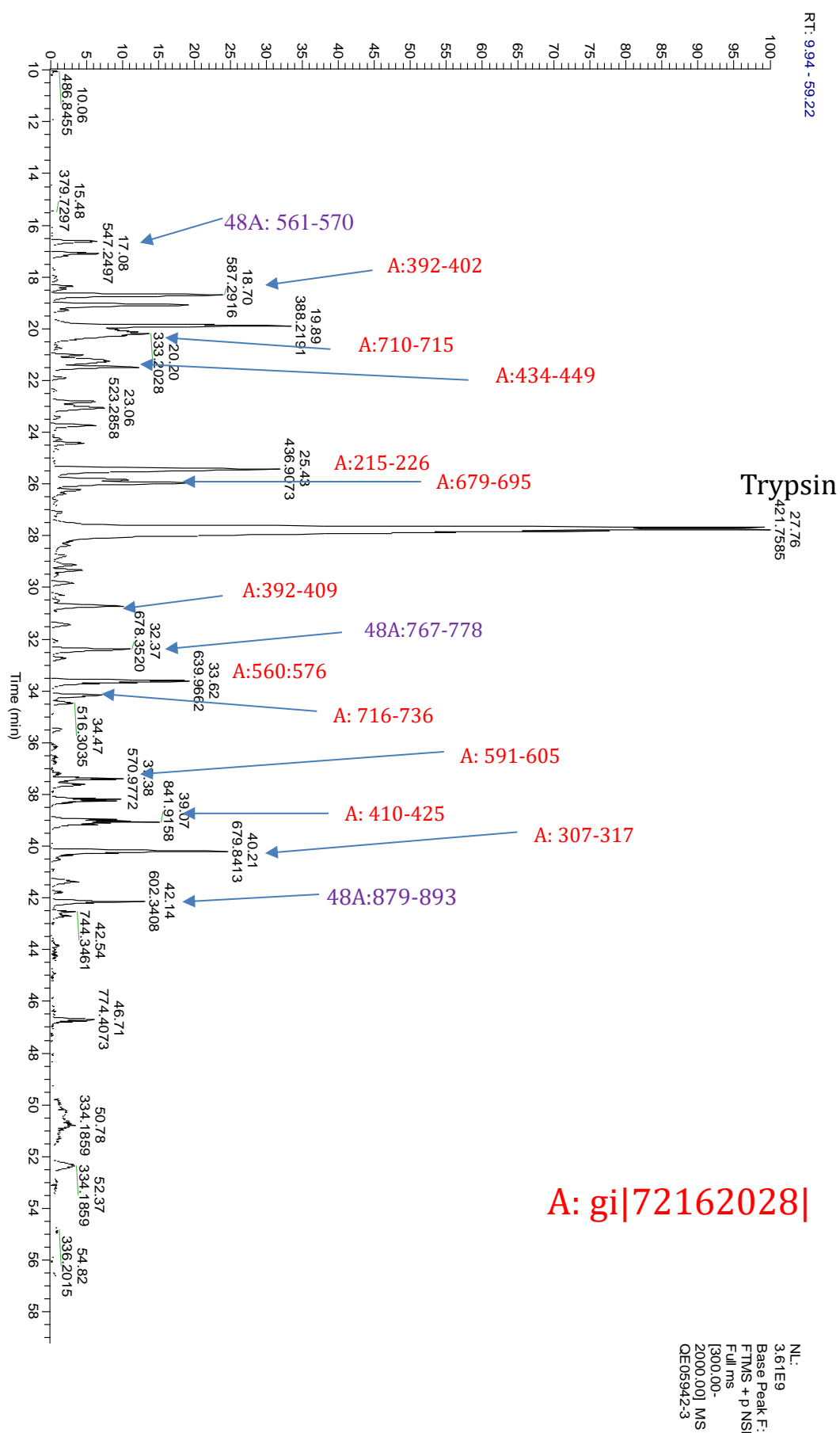


Figure 18.LC-MS result for the band at 102 kDa (Figure17) upper band

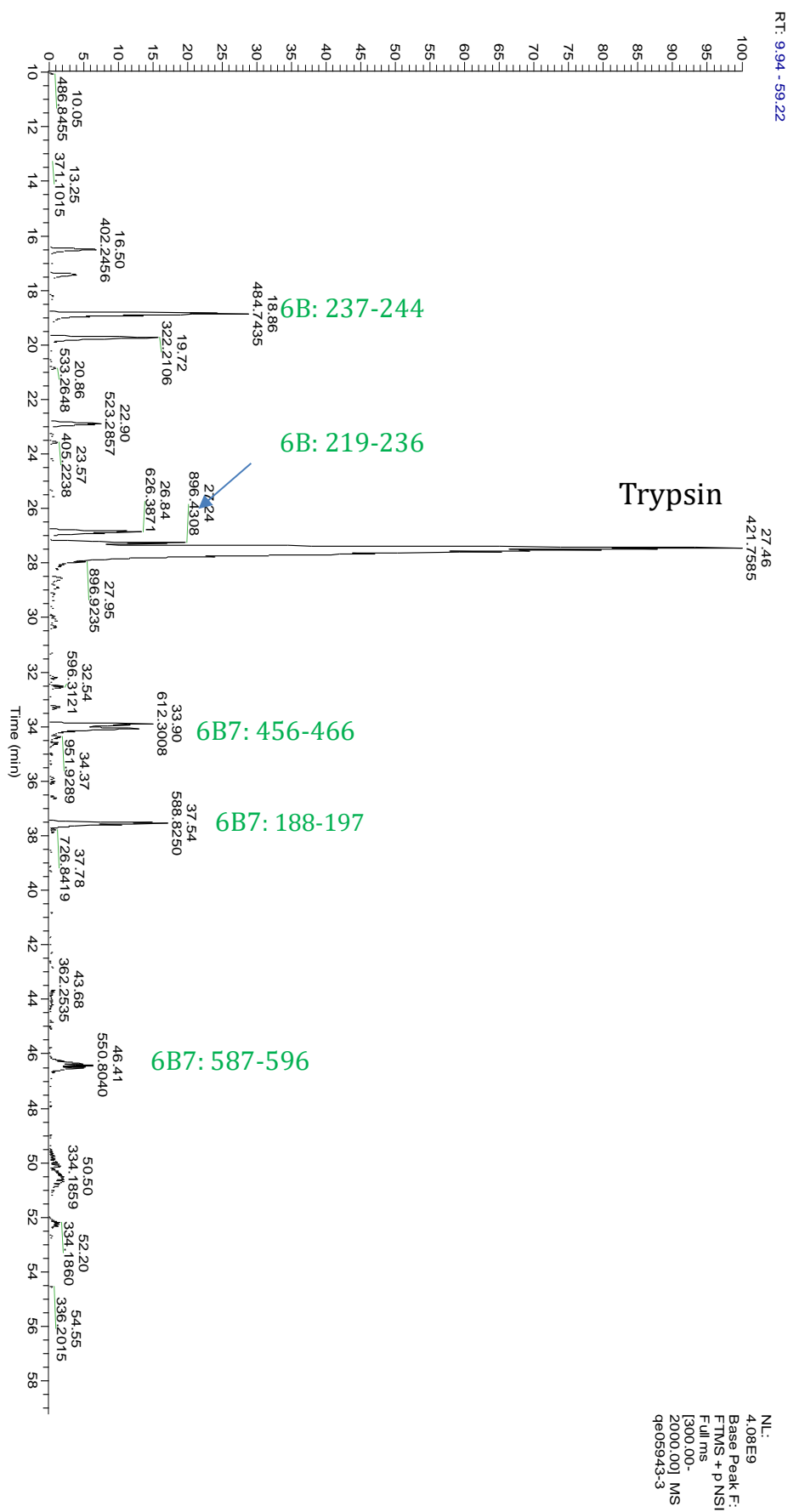


Figure 19. LC-MS result for the band at 65 kDa (Figure 17)

Count of sequence	Column Labels			
Row Labels	Gene name	Protein	102 kDa band	65 kDa band
gi 72162028	Tfu_1627	Cel9B	487	4
tr Q60029 Q60029_THEFU	Tfu_0620	Cel6B	52	308
tr Q47NH7 Q47NH7_THEF Y	Tfu_1959	Cel48A	143	3
gi 72162575	Tfu_2176	Cel9A	58	6
gi 72161398	Tfu_0994	Dihydrolipoyl dehydrogenase	21	6
gi 72162013	Tfu_1612	xyloglucanase	22	
gi 72161304	Tfu_0900	Cel5B	10	2
gi 72163322	Tfu_2923	Xyl10A	5	
gi 72162220	Tfu_1812	Putative peptide transport system substrate binding protein	4	
gi 72163039	rpsC	30S ribosomal protein S3	1	2
gi 72161478	Tfu_1074	Cel6A	3	
gi 72162050	Tfu_1649	Catalase	2	
gi 72160983	Tfu_0579	Serine peptidase	1	
Grand Total			809	331

Table 4. Spectral counts summary for trypsin digested protein samples analyzed via LC-MS/MS

3.3 Discussion

The secreted protein concentration in the supernatant of *T. fusca* culture is very dilute to begin with. For example, typically from a 4 liters *T. fusca* culture volume (using 4% CMC as carbon source) we recover 3.8 liters of supernatant broth with a protein concentration of ~0.06 mg/mL. Such a large volume is challenging to store and purify on a laboratory scale since most pre-packed FPLC column volumes range between 1-100 mL. As a result, after the fermentation was completed the first thing we did was to rapidly concentrate the protein from the supernatant for long-term storage. Before we scaled up the culture from 500 mL to 4 liters, we used Millipore 15 mL centrifugal filter units (Mol. Wt Cutoff 10 kDa, PES membranes, Millipore) to centrifuge our samples

for 40 minutes at 2800 rpm, which only gave us about 2.5 folds concentration, from 500 mL to 200 mL. However, a major drawback of this method is, due to the limited volume of the filter units readily available for bench scale biochemical separations in the lab, only 90 mL of supernatant could be centrifuged per run. This meant multiple runs of very time consuming centrifugation were necessary to achieve protein broth concentration. Therefore, in our case the ammonium sulfate precipitation method to rapidly recover and inexpensively concentrate the protein turned out to be a much more effective protein isolation strategy. However, when the concentration of ammonium sulfate exceeded 40% (w/v), the residual CMC carbon source in the culture broth would also co-precipitate with the protein. But if we stopped at 40%, though we might end up losing some of our protein in the broth, we could prevent co-precipitation of the CMC. In the future, other more efficient methods for crude enzyme recovery should be explored.

Before we used IEX for Cel6B polishing, the optimum conditions for protein purification such as strength of buffer, pH of buffer, flow rate and elution volume needed to be determined. Thus, 20 mM Tris HCl buffer was chosen as the starting buffer according to the manual of HiTrap Q column, which is also a widely used buffer for anion exchange. Also, 0.5 M NaCl was decided to be the ionic strength of elution buffer at first. The pI's of enzymes secreted by *T. fusca* range from 4.0 to 7.5, while Cel6B has a theoretical pI of 4.1. Thus, pH of buffers needed to be higher than pI's of protein to facilitate the positively charged desired protein to bind to the column. Here, we first tried a pH of 8 that is higher than the pI's of all major *T. fusca* cellulases expected in the crude mixture. When the increasing NaCl based gradient elution was started, proteins are expected to wash off from the column in the order of their binding strengths. Thus, proteins with higher pI's are expected to bind weakly to the column, thus should be

eluted first. That is also the reason why we suspect peak 1 from HiTrap Q corresponds to non-cellulolytic enzymes like xylanases which have a more basic pI than Cel6B. Peak 1 eluted first indicated that the enzymes in peak 1 had a higher pI, while also the low molecular weight and lack of detectable cellulase activity suggests that it is highly likely that the eluting proteins are xylanases like E13 (see Table 5). Peak 2 was the second peak eluted from the column, which suggested that enzymes in peak have a higher pI than peak 1 but lower than peak 3. From the SDS-PAGE we know that peak 3 should contains Cel6B and other cellulases that have a pI close to 4.1, which suggests that the pI of peak 2 could be likely between 5-6, which corresponds to endoglucanases Cel5A and Cel6A. Furthermore, the activity assays results also demonstrated that peak 2 contains mostly endo-enzymes. For CI/CIII assays, we saw a lower released soluble sugar in the supernatant-based activity on CI than CIII, which was expected for endo-enzymes. Also, the soluble reducing sugar is much lower than the insoluble reducing ends for both CI and CIII, which further suggests that there were mostly endolytic cuts generated in the insoluble cellulose pellet. Based on CMC activity assays, peak 2 also showed relatively high reducing sugar concentrations, which was an indication of endoglucanase activity. In these cases, we suspected that peak 2 contains endo-lytic enzymes, however this assumption would need to be verified further by proteomics analysis in the near future. For peak 3, we saw protein bands at 65 kDa that were likely arising due to Cel6B, however, several co-eluting proteins were also seen with the putative Cel6B proteins. The reason of the co-eluting could be that the pI's of the cellulases are very close to each other, and thus they can elute from the column at similar salt concentrations. Before we attempted to use other chromatography steps to get better separation among eluting cellulases in peak 3, we found that protein bands higher than 100 kDa seen originally in the crude enzymes were missing in peak 1 to

peak 3. Therefore, to check if these proteins were still bound to the IEX column, we used a sequentially higher salt concentration in the elution buffer. After the 0.5 M NaCl gradient elution step, we changed the step of gradient elution from 0.5 to 2 M NaCl (Figure 10). Interestingly, we got additional protein peaks 4, 5, 6 eluting from the column at higher salt concentrations. One of the initial eluting fractions was found to be enriched in Cel6B that was further polished using SEC. From SDS-PAGE we were able to confirm that the purified Cel6B fraction after SEC was >99% pure (based on image lab software based densitometric analysis for Cel6B band at 65 kDa).

Protein name (designation)	Accession no.	Theoretical M_r /pI	Exp M_r /pI
β -1,4-Exocellulase (Cel48A)	YP_290015	104/4.2	110/3.3 110/3.4 90/3.3 80/3.4 27/4.2
β -1,4-Endocellulase (Cel9B)	YP_289685	101/4.0	110/3.4 90/3.3 82/3.4 45/3.4
β -1,4-Endo/exocellulase (Cel9A)	YP_290232	90/4.4	110/3.7 34/4.2
β-1,4-Exocellulase (Cel6B)	YP_288681	60/4.1	65/3.4 44/4.1
β -1,4-Endoxylanase (Xyl10A)	YP_290979	49/4.9	45/4.7 42/4.1
β -1,4-Endoglucanase (Cel5A)	YP_288962	50/5.2	45/4.6
Putative cellulose-binding protein (E8)	YP_289723	47/4.4	42/4.1
β -1,4-Endoglucanase (Cel6A)	YP_289135	46/5.9	45/5.3 40/5.3
Putative secreted proteolytic enzyme containing NLPC_P60 domain (E9)	YP_289090	36/4.5	35/4.2
Putative secreted cellulose-binding protein (E7)	YP_289329	25/7.5	20/5.9 20/6.1 17/5.8 14/3.8
Putative secreted protein containing lytic transglycosylase and goose egg white lysozyme domain (E10)	YP_288519	23/4.2	26/3.3
β -1,3-Glucanase (Lam81A)	YP_290186	82/5.0	70/4.4
Predicted secreted aminopeptidase (E11)	YP_290459	49/4.5	57/4.0
Putative secreted proteolytic enzyme containing NLPC_P60 domain (E12)	YP_290318	42/4.9	40/4.7
Putative secreted xylanase or chitin deacetylase (E13)	YP_290845	27/6.7	27/5.8 27/6.1

Table 5. Identified *T. fusca* extracellular proteins when grown on cellobiose. Cel6B entries for theoretical and experimental measured pI/Mol.Wt values are highlighted in yellow here.

Table taken from Wilson, S. C. a. D. B., Proteomic and Transcriptomic Analysis of Extracellular Proteins and mRNA Levels in *Thermobifida fusca* Grown on Cellobiose and Glucose, *Journal of bacteriology*, 180, 6260–6265 (1998).

We made an unexpected finding during our HiTrap Q purification of Cel6B.

Interestingly when we collected protein fractions that contained Cel6B and ran it immediately after protein purification on the SDS-PAGE the same day, we found there were two bands very close to each other (Figure 12, lane 8), at 62 kDa and 67 kDa.

Next, after we flash froze that protein fraction enriched in Cel6B and stored it in the

freezer at -20°C , and then later after a week if the same fraction was thawed to run again on SDS-PAGE we surprisingly found a single new band at 65 kDa (figure 17, lane 3, 4, 5). This experiment was repeated several times using SDS-PAGE gels from different vendors; however, we always saw only one band at around 65 kDa after the freeze-thaw cycle. The results of LC-MS have also confirmed that this protein band is Cel6B, and not two different proteins. One possible explanation is that the distinct conformations of native Cel6B protein glycosylation are homogenized during the storage or freezing/thawing cycles. Protein glycosylation is known to impact electrophoresis of protein isoforms and could be the most logical explanation of this interesting phenomenon that has never before been reported in the literature for cellulases to the best of our knowledge.¹²

Chapter 4 Activity assays

4.1 Materials and methods

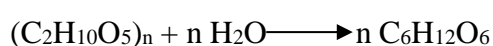
4.1.1 Crude enzyme assays

Phosphoric acid swollen cellulose (PASC), Avicel based cellulose-I (CI), and Avicel based cellulose-III (CIII) hydrolysis activity assays were used to test the overall cellulase activity of the isolated *T. fusca* culture broth supernatant. All enzyme activity assays were adapted to be conducted using scaled-down microplate-based methods as reported by Chundawat and others.^{3,19} Briefly, assays were conducted in 96-well round bottom microplates conducted in 200 μ L total volume that comprised of 80 μ L of 10 g/L CI/CIII or 100 g/L PASC substrate along with 100 μ L of 50mM pH 5 Na-acetate buffer. Next, 20 μ L of suitably diluted crude enzyme was added to each well to achieve different protein loadings (e.g., 2.5 or 5 mg total enzyme loading per gram of cellulose). DI water was added to reach the final volume 200 μ L when needed. After 24 hours of incubation at 55 °C with 5 rpm end-over-end mixing, the plates were centrifuged at 2000 rpm for 5 min. Next, 30 μ L of supernatant was removed and added to 60 μ L of 3,5-dinitrosalicylic acid (DNS) assay reagents in a 96-well PCR plate (Spectrum® PCR Plate). The plate was incubated at 95 °C in a thermal cycler (Eppendorf™ Mastercycler™ Nexus Thermal Cycler) for 5 min followed by cooling to 10 °C for 10 mins. Next, we removed 36 μ L of this mixture and transferred it in to a flat bottom 96-well microplate containing 160 μ L DI water to read the solution absorbance at 540 nm. The plot of varying glucose concentration-based standards curve was obtained to calculate reducing sugar concentration as glucose equivalent. Using the slope of the standard curve plot, the absorbances for unknown samples can be converted to mgs of reducing sugar (glucose equivalent). From this value one can calculate the percent

conversion of original cellulose added in to glucose equivalents produced using the formula provided below;

The formula was derived based on cellulose added in each well and the factors used to convert 1 mole of cellulose into glucose equivalents:

X is the amount of cellulose that has converted to reducing sugars and n is the degree of polymerization of cellulose. For microcrystalline Avicel used in this study, this value is close to 200 units.²⁰



n162 g

n(180)

X

Reducing sugar concentration in each well *0.2(mL)

Then $x = 0.9 * 0.2 \text{ mL} * \text{reducing sugar concentration}$, percent conversion = $x / \text{amount of cellulose in mixture at } t=0$

Also, the background noise was subtracted using the protein-only and cellulose-only blank controls. Crude enzyme assays were also set up to determine the optimum pH and temperature for the *T. fusca* crude enzyme system in our setup. Crude *T. fusca* enzymes were buffer exchanged into 10 mM MES buffer (pH 6.5) containing 25 mM NaCl, and 1 µg total enzyme was added to each microwell to achieve a 2.5 mg/g cellulose total protein loading. Next, 40 µL of 10 g/L PASC and 20 µL of 1 M MES, at varying pHs, along with 500 mM NaCl were added along with DI water to makeup the 200 µL total reaction volume, the effective concentration in each well were 100 mM MES, 50 mM NaCl. For pH dependence assays, we tested pH between 5.5-7 (at 0.5 pH unit increments) using MES as the buffering reagent with all assays performed at 55 °C or 24 hours. For temperature dependence, a fixed pH 6.5 MES buffer was used, the assays were performed at 50 °C / 55 °C / 60 °C / 65 °C for 24 hours. After 24 hours,

30 μ L supernatant was removed and total reducing sugars were measured using the standard DNS assay method.

4.1.2 Purified Cel6B activity assays

PASC based pH dependence assay: PASC substrate-based pH dependence assays were conducted for purified Cel6B at 1 mg/g cellulose protein loading at 55°C for 24 hours. The purified proteins were buffer exchanged in to a buffer containing 10 mM MES and 25 mM NaCl. For the activity assays, 20 μ L of 1M MES, 25mM NaCl at different pHs were added in to the microwells containing 40 μ L of 10 g/L PASC, the effective concentration here is 100 mM MES, 2.5 mM NaCl, DI water was used to make the final volume 200 μ L. CMC based assays were done at 2.5 mg/g cellulose total protein loading at 55 °C for 4 days, the effective composition in each well was the same as described in PASC assay above.

Next, p-nitrophenyl- β -cellobioside (pNPC) based activity assays were performed at 50 °C for 24 hours in a thermomixer (Eppendorf Thermomixer C). Here, 2 μ g of purified Cel6B was added in to a flat bottom 96-well microplate containing 100 μ M pNPC along with 20 μ L 1M Na-Acetate buffer at pH 5.5. Additional DI water was added to make the volume 200 μ L. After 24 hours, 100 μ L 0.1 M NaOH was added into the wells to arrest the reaction, and solution absorbances were read at 410 nm.

Avicel based CI/CIII hydrolysis assays using 0.1125 mg/g cellulose total protein loading were performed at 60°C for 24 hours, the percent conversions were calculated the same method as described in chapter 3.

4.1.3 Synergism assay on CI and CIII

To create endolytic cuts on the insoluble cellulose chains, CelE and CelE-CBM3a were used and compared to pick a suitable endocellulase construct for further assays. CelE is a GH5 endocellulase while CBM3a is a Type-A cellulose-binding module from *Clostridium thermocellum*. Details about how to prepare these enzymes are provided in another published study by Chundawat and coworkers elsewhere.²¹ Ideally, after reaction with the endo-enzyme, the endo-enzyme that is bound to the cellulose pellets should be washed off from the cellulose chain via several buffer washes of the reacted pellet. This is to prevent any leftover endo-cellulase from interfering along with the Cel6B added in the subsequent ‘re-start’ based hydrolytic assays. This ‘re-start’ assay was setup to systematically test our hypothesis that endo-cellulases can create endolytic cuts on cellulose chain and are ultimately responsible for the increased activity seen for *T. fusca* exocellulases like Cel6B on cellulose-III.

Different protein loadings of CelE and CelE-CBM3a ranging from 10 mg/g to 200 mg/g cellulose were added to a round bottom microplate containing 40 μ L of 10 g/L CI or CIII, along with 0.1 M MES pH 6.5 buffer to make up the final reaction volume to 200 μ L. The microplates were incubated at 60°C for 24 hours in end-over-end mixing oven at 5 rpm. After 24 hours, the plate was centrifuged at 2000 rpm for 5 minutes, and the supernatant was removed by pipetting followed by SDS-PAGE, DNS assay, and Bradford assays for the supernatant. Next, 150 μ L of 0.1 M MES buffer at pH 6.5 was added into the microwell that had treated cellulose pellet inside, mixed well by pipetting, then centrifuged followed by removal of the supernatant were removed that was then discarded. The washing steps were repeated 6 times, and the cellulose pellet samples were taken after the second, fourth, and sixth washing steps for SDS-PAGE

analysis to check for residual proteins bound to the cellulose.

After the final washing step was completed, the volumes of the washed endocellulase treated pellets were adjusted back to make up the volume to 40 μ L using DI water. Desalted Cel6B and 20 μ L 1 M MES, 500 mM NaCl, at pH 6.5 was then added to all microwells and DI water was used to make up the final volume to 200 μ L to 're-start' enzymatic hydrolysis. The plates were then incubated at 60°C in end-over-end mixing oven at 5 rpm. After 24 hours, the plates were centrifuged at 2000 rpm for 5 minutes, and 30 μ L of the supernatant was removed and analyzed using the DNS assay method. The percent conversions were also calculated from the reducing sugar concentration as before.

4.2 Result

4.2.1 Crude enzyme assays result

T. fusca crude enzyme secretomes enriched in cellulases are very active on PASC, and within 72 hours, all protein loadings achieved 100% conversion of cellulose into soluble sugars like glucose/cellobiose (Table 6). Shorter time points of 2 hours and 4 hours were also assayed. After 2 hours, at 5 mg/g protein loading the crude enzymes achieved ~33% conversion while at 10 mg/g protein loading ~38% conversion was achieved. After 4 hours, both of protein loadings achieved ~50% conversion.

For 5 mg/g enzyme loading during CI/CIII hydrolysis assays, there was an increasing trend of activity from 24 (data reported) to 120 hours (data not shown), but the difference between CI and CIII as marginal. However, for 10 mg/g enzyme loadings, higher activity was seen for CIII for all time points (24 hr data reported).

24 hr samples for various enzyme loadings activity on PASC substrate	PASC (5mg/g)	PASC (10mg/g)	PASC (25mg/g)	PASC (50mg/g)
%cellulose –to-soluble sugars yield	79.65%	92.8%	100%	100%
Reducing sugar conc. (mg/mL)	3.54	4.13	4.77	4.77
Standard error	0.06	0.06	0.05	0.07

Table 6. Crude enzyme activities on PASC substrate for varying enzyme loadings and 24 hr timepoints

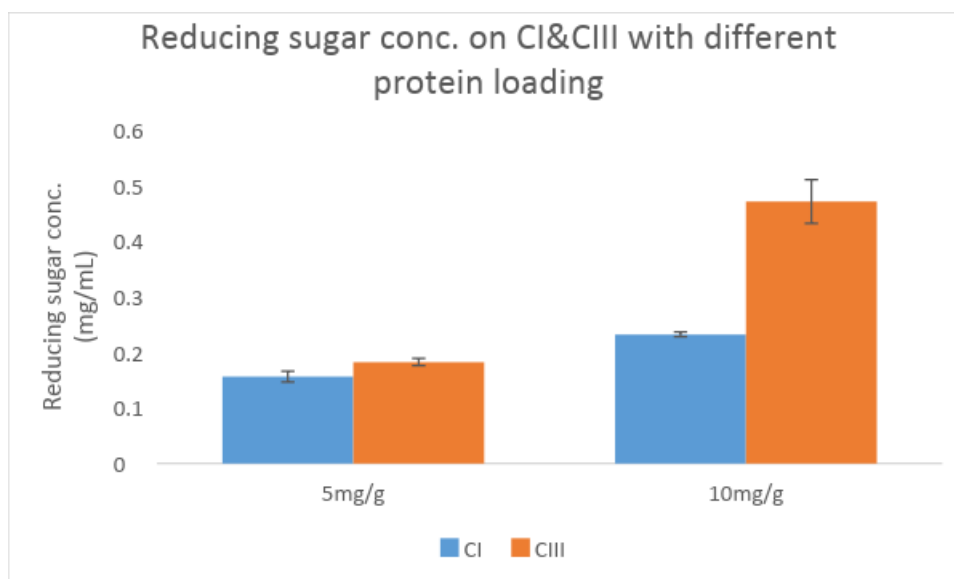


Figure 20. Crude enzyme activity on CI & CIII. DNS assay conducted on soluble sugars released. 24 hrs cellulose hydrolysis time points are shown here alone.

Crude enzyme pH dependence assays were done at pH 5.5, pH 6, pH 6.5, and pH 7 conditions. After 24 hours, pH 5.5 and pH 6 showed the highest cellulase activity giving ~14.5% conversion to soluble sugars each. For temperature dependence assays, the hydrolysis activity reached a maximum percent conversion of 11.3% at 65°C.

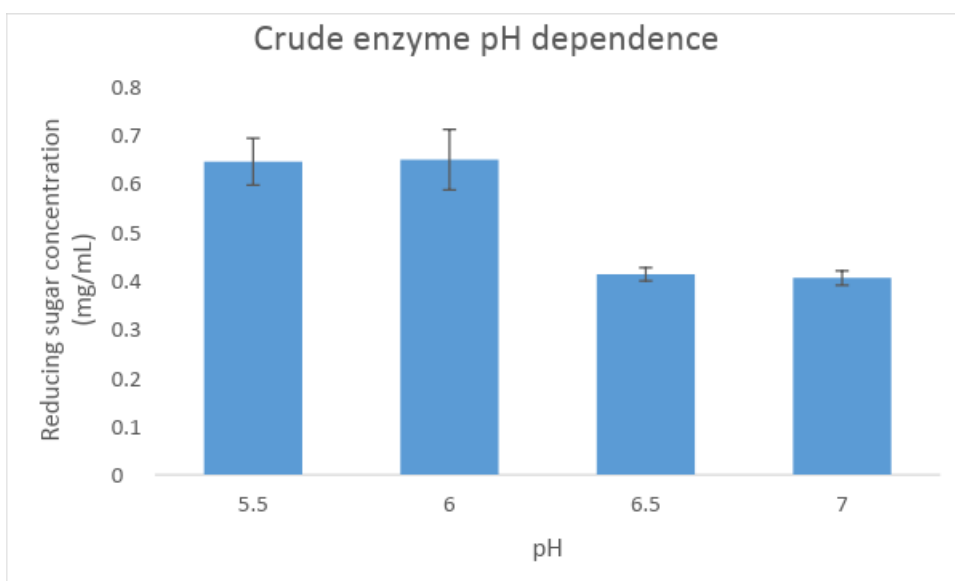


Figure 21. Crude enzyme pH dependence

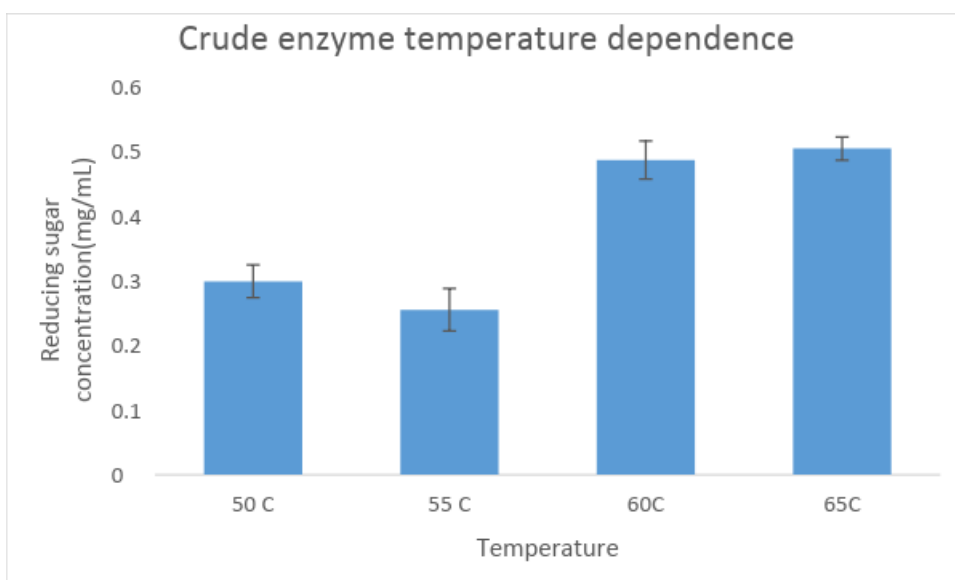


Figure 22. Crude enzyme temperature dependence

4.2.2 Purified Cel6B assay

The pH dependence assays for purified Cel6B were conducted at pH 5.5, pH 6, pH 6.5, and pH 7. The percent conversions were calculated from the reducing sugar concentration estimated from the DNS assay. From the crude enzyme pH dependence assay, we know that at both pH 5.5 (and 6), the crude enzymes gave the highest percent conversions. However, after 24 hours, the microwells under pH 6.5 showed higher percent conversion of ~4.7% (Table 7), while pH 5.5 gave lower percent conversion of

~3%. Also, 2.5 mg/g protein loading during PASC assays incubated for 4 days gave a percent conversion ~16.4%. For the same reaction conditions, pure Cel6B gave ~2.1% conversion on CMC, which is lower compared to PASC activity. This result is not surprising considering Cel6B is an exo-enzyme, and because CMC is partially chemically modified cellulose, Cel6B therefore has significantly lower activity on modified celluloses like CMC unlike PASC. Also, the purified Cel6B did not show any activity on pNPC. These results further demonstrate that our purified Cel6B sample did not have any significant endocellulases contamination, which was also independently confirmed via proteomics analysis.

PH DEPENDENCE	5.5	6	6.5	7
CONC.(MG/ML)	0.13	0.19	0.21	0.54
STANDARD ERROR	0.01	0.01	0.01	0.02
% CONVERSION	2.98%	4.27%	4.67%	3.77%

Table 7. Purified Cel6B pH dependence assay

The result of CI and CIII assays are tabulated in Table 8. There was an increasing activity trend seen for both CI and CIII within 120 hours with the maximum conversion (~19.2%; data not tabulated) reached for CI at 120 hours. Besides, much higher activity was observed on CI compared to CIII, which again supports our original hypothesis that increased endocellulase activity is needed and likely responsible for the increased overall cellulase cocktail activity on CIII.

	CONC.(MG/ML)	STANDARD ERROR	%CONVERSION
CI	0.34	0.03	7.72%
CIII	0.10	0.01	2.30%

Table 8. CI/CIII assay with purified Cel6B alone after 24 hrs

4.2.3 CelE and CelE-CBM3a binding and activity to create endo-cuts on cellulose

First, 100 mg/g and 200 mg/g protein loadings of CelE were tried out with CI and CIII. After 24 hours reaction, the supernatants were run on SDS-PAGE to observe the unbound proteins (Figure 23 and 24). From figure 23, comparing Lane 2 with Lane 3, it is clear that Lane 3 had less protein in the supernatant, which suggests most of the CelE-CBM3a was still bound to cellulose. However, comparing Lane 2 with Lane 6, Lane 3 with Lane 7, Lane 6 and lane 7 shows that lesser protein was in the supernatant, which suggests for both CelE and CelE-CBM3a, that more enzymes were bound to CIII than CI (likely still catalytically engaged with the substrates). Next, comparing 100 mg/g protein loading lanes with 200 mg/g protein loading lanes, we see more unbound protein in the 200 mg/g protein loading supernatant, which suggests we significantly loaded more protein than needed for the 200 mg/g protein loading assay. One possible reason could be the saturation of available active or binding sites on the cellulose surface. Also, the supernatant was taken for DNS assay to estimate the total hydrolysis activity, however, the microplate assays gave no reading at these initial cellulose loadings. From the SDS-PAGE results we know that the enzyme was binding to cellulose, however, it's likely that the DNS assay did not show any result if the soluble reducing sugar concentration in the supernatants was too low to be detected (<0.01-0.05 mg/ml). To address this problem, we decided to increase the amount of CI/CIII substrate in each well from 0.8 mg to 4 mg. When we increased the amount of CI/CIII, after the hydrolysis, even if we got the same percent conversion, the absolute reducing sugar concentrations should be at least 5-fold higher than before (to achieve equivalent % conversions).

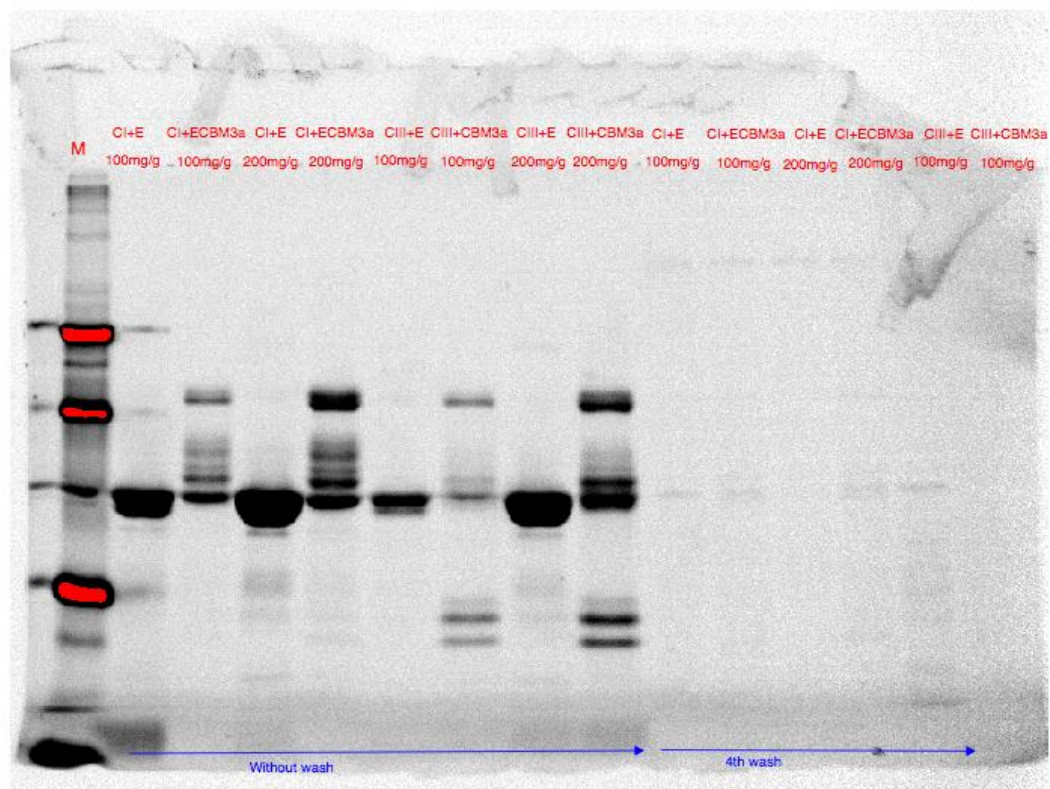


Figure 23. Stain-free SDS-PAGE of CelE and CelE-CBM3a reaction mixture supernatants

(Lane1: marker; Lane2-Lane9: reaction sup without wash. Lane2:CI+CelE, 100mg/g; Lane3:CI+CelECBM3a 100mg/g; Lane4:CI+CelE 200mg/g; Lane5:CI+CelECBM3a 200mg/g; Lane6: CIII+ CelE 100mg/g; Lane7: CIII+CelE 100mg/g; Lane8: CIII+CelECBM3a 100mg/g; Lane9: CIII+CelECBM3a 200mg/g; Lane10-Lane15: reaction sup after 4th wash; Lane10:CI+CelE 100mg/g; Lane11:CI+CelECBM3a 100mg/g; Lane12:CI+CelE 200mg/g; Lane13: CI+CelECBM3a 200mg/g; Lane14:CIII+CelE 100mg/g; Lane15:CIII+CelECBM3a 100mg/g;)

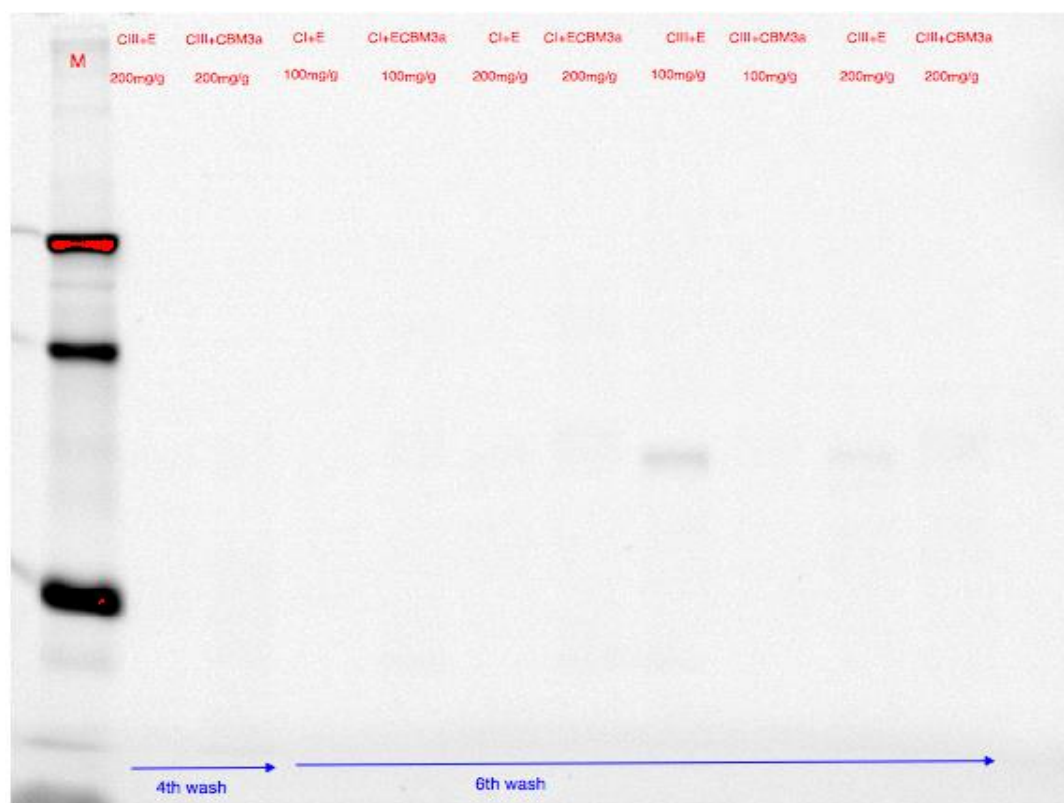


Figure 24. Stain-free SDS-PAGE of CelE and CelE-CBM3a reaction mixture washed pellets

(Lane1: marker; Lane2-3: 4th washed sup; Lane 2:CIII+CeE 200mg/g; Lane3: CIII+CeECBM3a 200mg/g. Lane4-11: 6th washed sup; Lane4: CI+CeE 100mg/g; Lane5: CI+CeECBM3a 100mg/g; Lane6: CI+CeE 200mg/g; Lane7:CI+CeECBM3a 200mg/g; Lane 8:CIII+CeE 100mg/g; Lane9:CIII+CeECBM3a 100mg/g; Lane10: CIII+CeE 200mg/g; Lane11:CIII+CeECBM3a 200mg/g)

Next, 10 mg/g, 50 mg/g, and 100 mg/g protein loadings of CelE and CelE-CBM3a were added to CI/CIII hydrolysis assay (with a 4 mg cellulose substrate per well). After 24 hours incubation, the supernatant was removed and 30 μ L of the supernatant and washed pellet were taken for DNS assays (Figure 25). Unfortunately, we lost the CI+CeE 50 mg/g samples and CI+CeE CBM3a 10 mg/g samples during handling, but final conclusions could still be drawn based on the remaining sample results. From the DNS results for the supernatant, an improved activity was observed for 50 mg/g protein loading compared to 10 mg/g protein loading, while 50 mg/g and 100 mg/g protein loading gave about the same activity. Therefore, 50 mg/g protein loading was picked for creating endo-cuts on cellulose for all future synergistic assays. Also, the 5th washed and 10th washed pellet were taken for SDS-PAGE analysis. We find that after 5 washes there were no detectable enzymes bound on cellulose for CelE, while after 10 washes

CelE-CBM3a is still tightly bound on the cellulose. Thus, CelE alone was used for creating endo-cuts on cellulose for future ‘re-start’ based synergistic assays with Cel6B. This was to avoid complications from residual unbound CelE-CBM3a interfering with our downstream Cel6B restart hydrolysis assays.

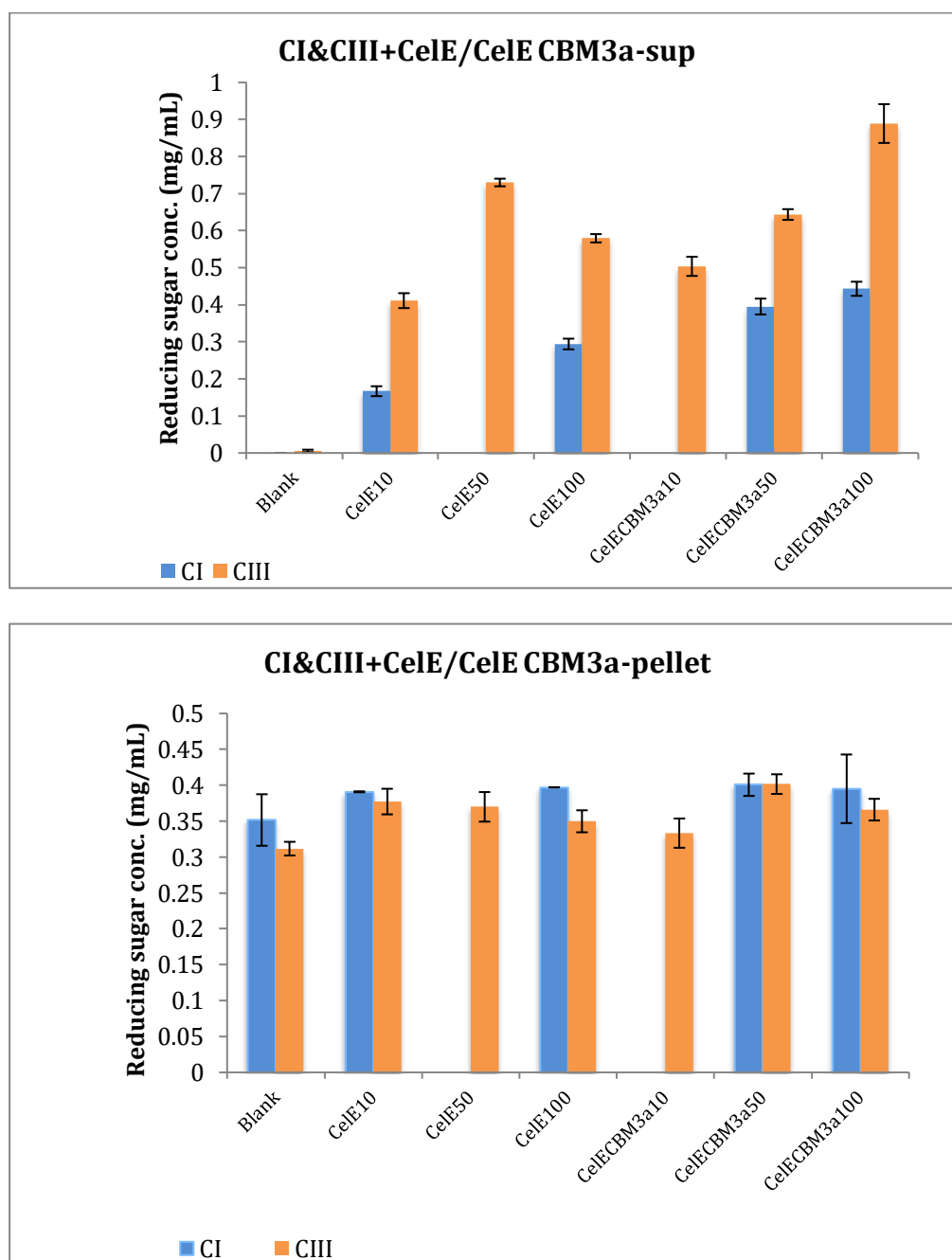


Figure 25. DNS result for CI&CIII and CelE/CelE CBM3a hydrolysis assay. (10,50, 100 means 10mg/g, 50mg/g and 100mg/g protein loading)

Top: DNS result for the supernatant. Bottom: DNS result for the insoluble pellet.

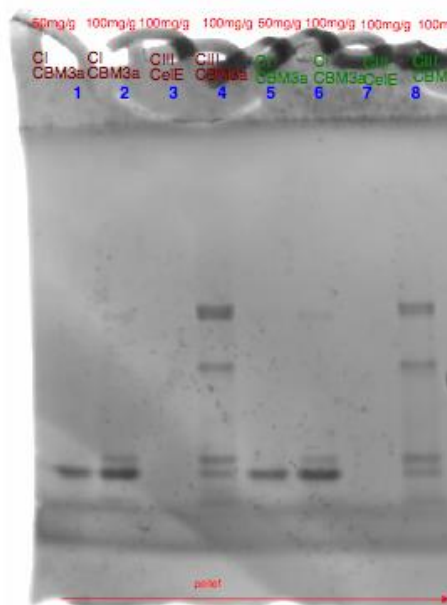


Figure 26. Coomassie stained SDS-PAGE of CelE/CelE-CBM3a+CI/CIII assay pellet.

(Lane1-4: 4th washed pellet. Lane1,2: CI+ CelE CBM3a 50mg/g, 100mg/g. Lane3: CIII+CelE 100mg/g. Lane4: CIII+CelECBM3a 100mg/g. Lane5-8: 10th washed pellet. Lane5,6: CI+ CelE CBM3a 50mg/g, 100mg/g. Lane7: CIII+CelE 100mg/g. Lane8: CIII+CelECBM3a 100mg/g.

4.2.4 Synergism assay with Cel6B

After CelE was added to CI/CIII and incubated for 24 hours, the supernatant of the reaction mixture was taken for DNS assay. The CI supernatant had a reducing sugar concentration of 0.19 mg/mL, which is equivalent to 4.30% conversion, while the CIII supernatant had a reducing sugar concentration of 0.36 mg/mL, which is equivalent to 8.03% percent conversion. As expected, CelE as a GH5 family endocellulase, showed overall increased activity on CIII than CI at 50 mg/g cellulose based enzyme loading.

Cel6B 'restart' based synergism assay results are shown in Figure 27 for CelE endo-cut and washed cellulose pellets. First, for 0.1125 mg/g protein loading, the difference between CI and CIII was marginal, one possible reason could be that the enzyme loading of Cel6B was too low to see a clear difference (possibly due to non-specific binding of the enzyme with the tube walls etc). On the other hand, for 0.225 mg/g

enzyme loading, there was a clear increase in activity for both CI and CIII. Also a higher percent conversion of 17% was seen for CIII at the higher enzyme loading, while 12% conversion was seen for CI, which indicated that adding Cel6B to the CelE treated cellulose substrate, it was possible increase the ‘re-start’ Cel6B exocellulase hydrolysis activity for CIII compared to CI allomorph.

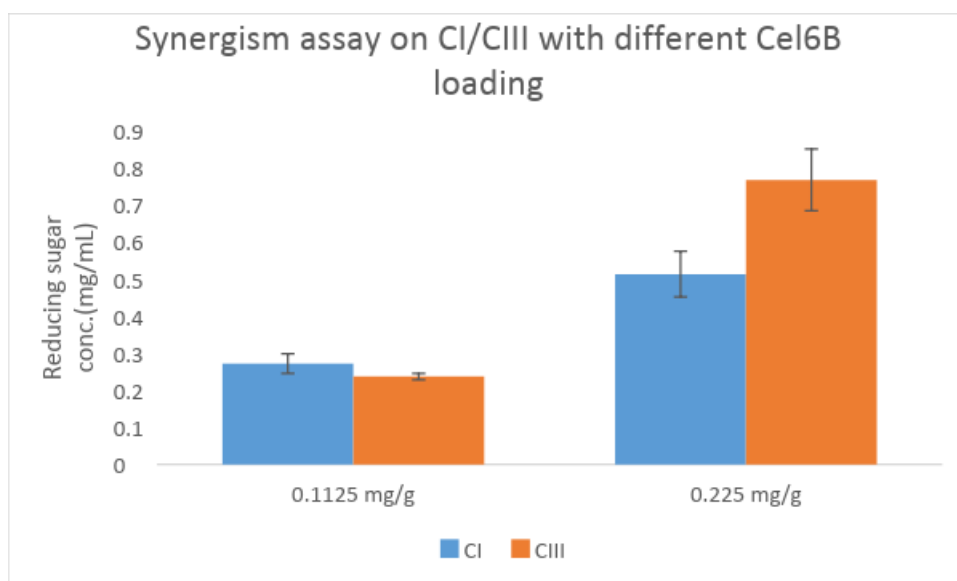


Figure 27. Synergism ‘re-start’ hydrolysis activity assay on endo-treated CI/CIII using Cel6B

4.3 Discussion

From the crude enzymes assay on CI and CIII, there was an enhanced activity on CIII seen for the crude cellulases cocktail secreted by *T. fusca*, similar to previous reports for *T. reesei* crude cellulases. However, a lower activity was seen on CIII for isolated pure Cel6B in the pure Cel6B hydrolysis assay. A similar lower activity has been reported by Chundawat and co-workers for *T. reesei* fungal derived processive exocellulases (e.g., CBH I or Cel7A and CBH II or Cel6A) on CIII versus CI. Cel6B as an exocellulase also showed lower activity on CIII than CI, this result makes sense based on the hypothesis that endocellulases are critical for the enhanced activity on CIII. Research is currently ongoing to elucidate the molecular mechanisms responsible for the reduced processivity of exocellulases on CIII using suitable single-molecule motility assays for engineered enzymes. Nevertheless, to further test our endo-exo

synergy hypothesis to explain the higher activity for crude cellulase mixtures on CIII, 'restart' synergism assays using Cel6B and an endocellulases CelE were designed. Here, we used CelE to first create endo-cuts on the surface of cellulose, then removed CelE from the system, and restarted the hydrolysis for the endo-cut CI/CIII using purified Cel6B alone to clearly provide supporting evidence for our endo-exo synergy hypothesis. From our synergism assay results, we can clearly see that Cel6B and CelE have to work together to significantly enhance hydrolytic activity for both CI and CIII, and that this enhancement in activity was found to be greater for CIII. This result agrees well with our proposed hypothesis.

Before we started the activity assays in Chapter 4, the effective composition in each well was set up to 100 mM MES, 50 mM NaCl in 200 uL reaction volume. The protein used in the assays were buffer exchanged to 10 mM MES, 25 mM NaCl, thus the buffer strength of the protein solutions should be low compared to the well, so that the impact of adding protein solutions to the reaction wells could be negligible on the effective buffer composition. The pH and effective buffer strength should be controlled for all activity assays. However, when we set up the synergism assay and purified Cel6B assay on CI/CIII, the effective concentration in the reaction wells was mistakenly set up as 100 mM MES, 2.5 mM NaCl. Thus, the protein volume added likely impacted the final salt concentration in the reaction well under this circumstance. Unfortunately, we did not have enough time to set up this assay again with the right effective concentration for this thesis project, but the results of the synergistic assays and purified enzyme assays on CI/CIII are still representative of the key results reported in this study. We do not expect our key findings would be altered by this minor change in buffer salt composition. If additional protein loading/ reaction time assay will be set up in the near

future, this assay would ideally need to be set up again to closely compare the effect of desired effective buffer/salt concentrations on *t. fusca* cellulase activities.

Chapter 5. Future Studies and Conclusions

In this project, we obtained an enhanced endo-exo synergistic activity on pretreated CIII for bacterial cellulases secreted by *T. fusca*, which was similarly seen for fungal cellulases in a previous study. An increased activity on CIII was also seen for *T. fusca* crude enzymes and another bacterial endocellulase CelE, thus providing additional supporting evidence that enhanced endo-activity is responsible for the overall increased cellulase crude cocktail activity on CIII. Besides, with a relatively low enzyme loading of Cel6B (0.225 mg/mL), a 15% absolute higher cellulose-to-soluble sugars conversion was seen for endo-cellulase treated CIII than when CelE alone was used, which again demonstrates the importance of studying cellulase synergism.

However, there are some additional experiments that will need to be completed in the near future. First, synergistic assays will need to be run under a range of effective buffer and salt concentrations to compare results with other published studies. From our assay results, we saw that 0.1125 mg/g Cel6B loading was too low to give any significant synergistic activity for CelE treated CI or CIII, therefore higher protein loadings up to 2 mg/g should be considered for future synergistic assays. Also, longer time points of 48 hours and 120 hours need to be included as well to study extent of maximum conversion possible for both cellulose allomorphs.

Second, to further solidify the hypothesis that the enhanced overall activity of pretreated CIII stems from enhanced endo-exo synergy activity for enzymes secreted by *T. fusca*, endo-enzymes isolated from *T. fusca* crude enzymes directly could also be used instead of CelE. This study could further verify that if the endocellulases from different organisms can provide the same degree of synergy compared to endocellulases isolated

from same organism. In previous study of endo-exo synergism,¹⁶ more efficient hydrolysis activity was found when one endocellulase was included along with two exocellulases that target both reducing and non-reducing cellulase chain-ends. It would be therefore interesting to further investigate into the synergy among more than two endocellulases and exocellulases mixtures that could specifically hydrolyze CI/CIII and create new sites for access to other enzymes. This could probably lead to additional enhanced activity than currently seen in our simplified two cellulases based endo-exo synergistic assay.

Lastly, after a thorough study of *T. fusca* enzymes activity, to further test if bacterial cellulases showed improved endo-exo synergistic activity on cellulose-III, it would be interesting to studying activities of cellulolytic enzyme cocktails from other organisms as well to verify if this phenomenon for improved endo-exo synergy on CIII is still seen. These studies will ultimately have an important bearing on the choice of cellulolytic organisms and enzyme cocktail composition chosen for conversion of ammonia-pretreated lignocellulosic biomass to fermentable sugars in biorefineries.

Appendix

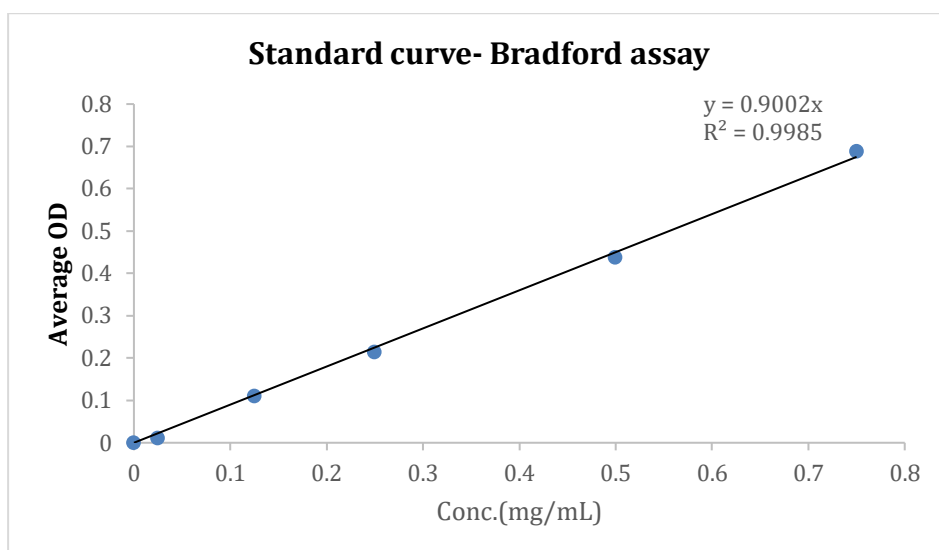


Figure A 1. Bradford assay standard curve for *T. fusca* growth curve

Obtained from different concentrations of BSA standard solution (Bio Basic) :0.025 mg/mL, 0.125 mg/mL, 0.25 mg/mL, 0.5 mg/mL, 0.75 mg/mL.

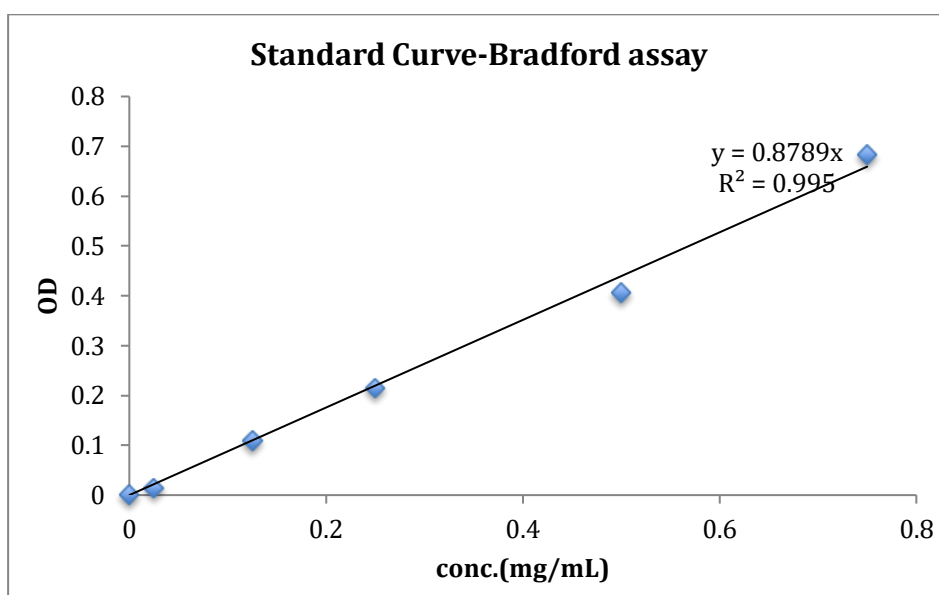


Figure A 2. Bradford assay standard curve for optimizing temperature and pH

Obtained from different concentrations of BSA standard solution (Bio Basic) :0.025 mg/mL, 0.125 mg/mL, 0.25 mg/mL, 0.5 mg/mL, 0.75 mg/mL.

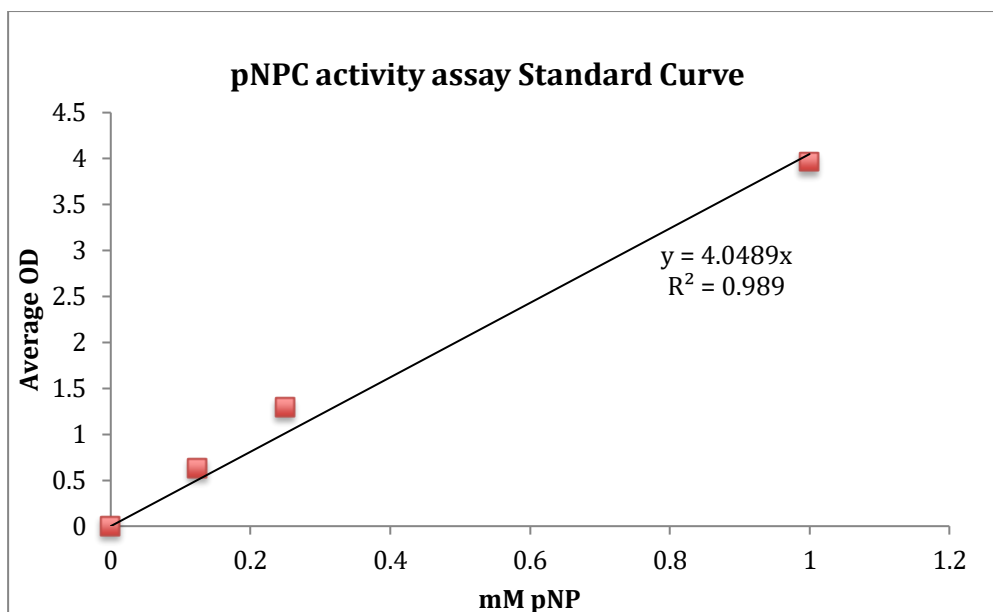


Figure A 3. pNPC activity assay standard curve

Obtained from different concentrations of para-Nitrophenol (pNP) standard solutions (MP Biomedicals): 0.1125 mM, 0.25 mM, 0.5 mM, 1 mM, 2 mM.

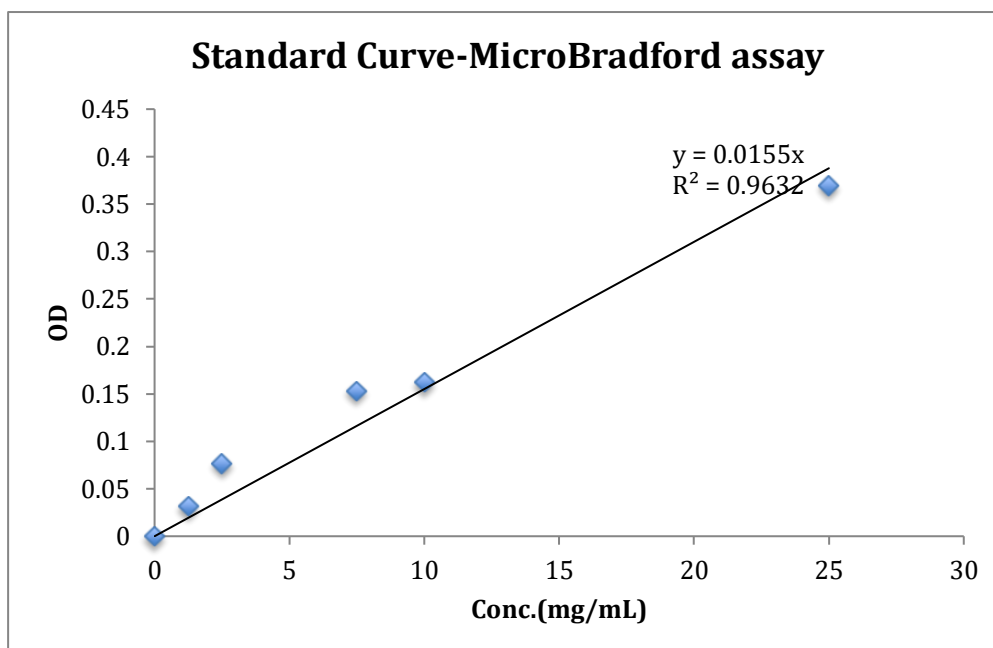


Figure A 4. MicroBradford assay standard curve

Obtained from different concentrations of BSA (Bio Basic) standard solutions: 1.25 $\mu\text{g/mL}$, 2.5 $\mu\text{g/mL}$, 5 $\mu\text{g/mL}$, 7.5 $\mu\text{g/mL}$, 10 $\mu\text{g/mL}$.

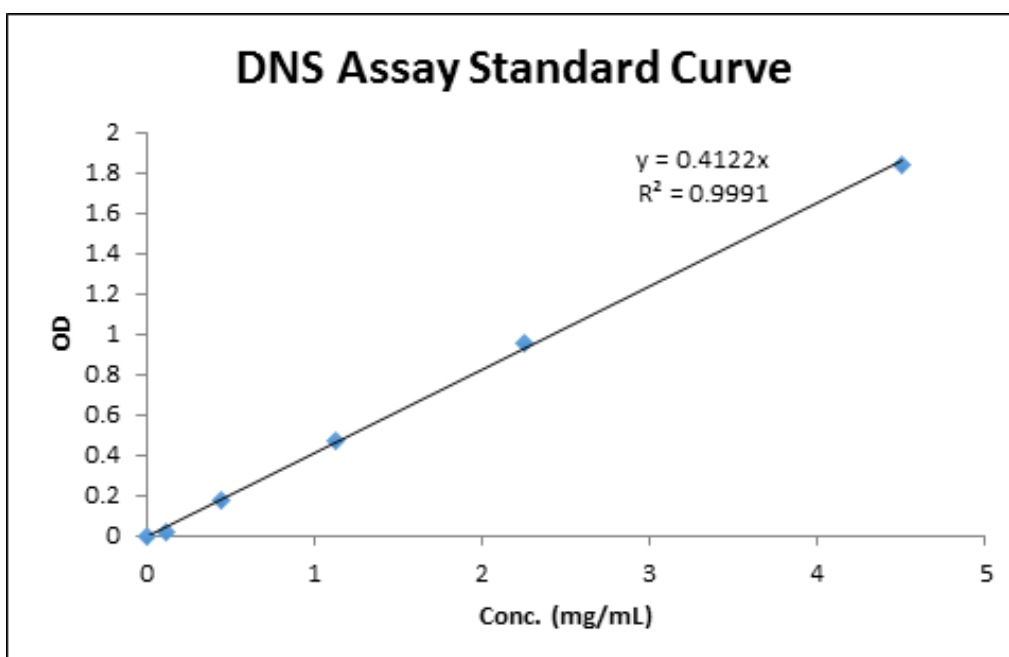


Figure A 5. DNS Assay Standard Curve for Activity Assays on HiTrap Q Fractions.

Obtained from different concentrations of glucose standard solutions: 0.1125 mg/mL, 0.45 mg/mL, 1.125 mg/mL, 2.25 mg/mL, 4.5 mg/mL.

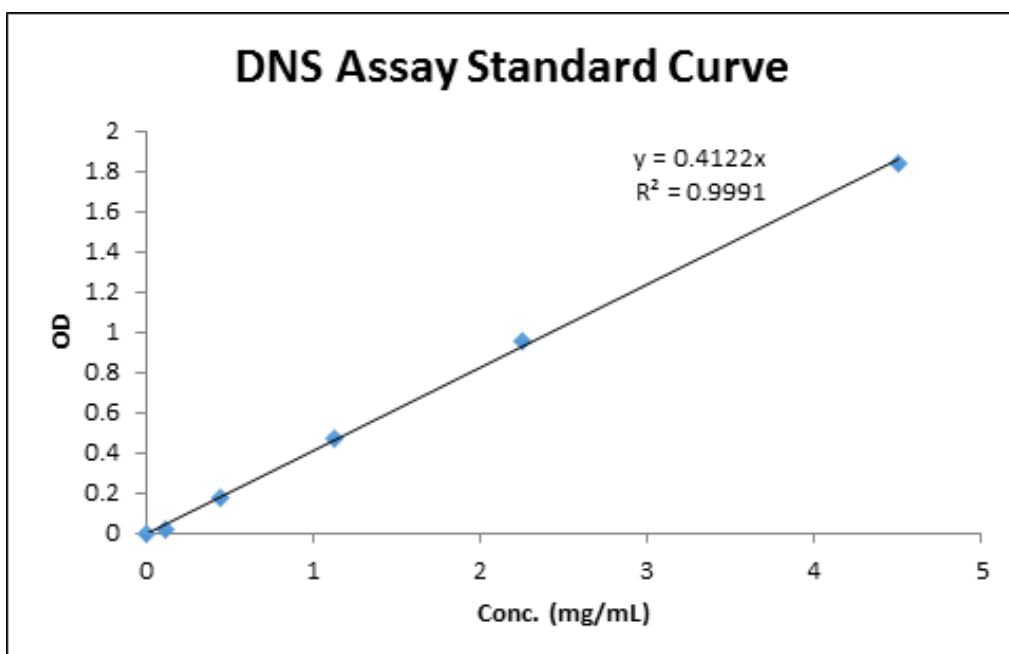


Figure A 6. DNS Assay Standard Curve for activity assays on Crude enzymes

Obtained from different concentrations of glucose standard solutions: 0.1125 mg/mL, 0.45 mg/mL, 1.125 mg/mL, 2.25 mg/mL, 4.5 mg/mL.

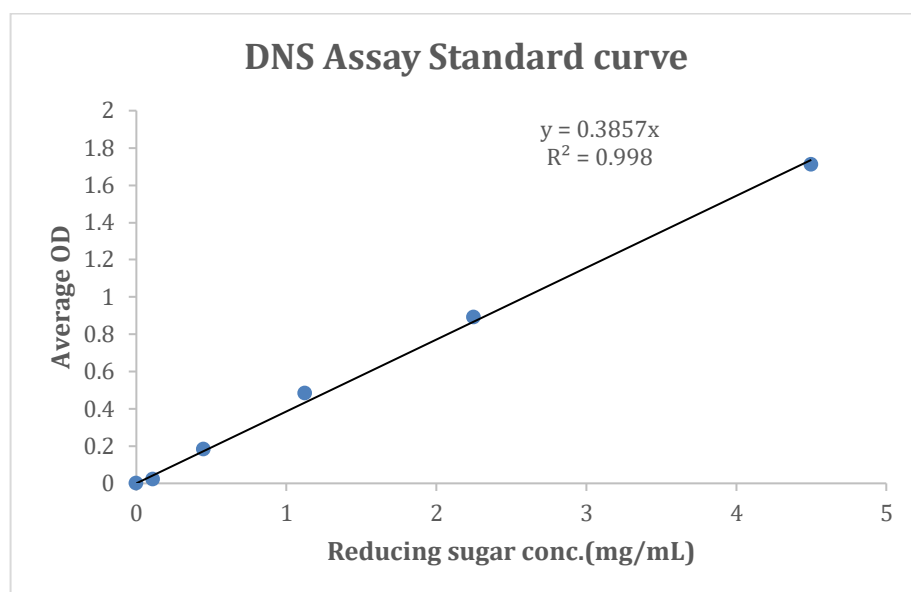


Figure A 7. DNS Assay Standard Curve for Activity Assays on Purified Cel6B and synergism assays

Obtained from different concentrations of glucose standard solutions: 0.1125 mg/mL, 0.45 mg/mL, 1.125 mg/mL, 2.25 mg/mL, 4.5 mg/mL.

Bibliography

1. Sousa, L. *et al.* Next-generation ammonia pretreatment enhances cellulosic biofuel production. *Energy & Environmental Science* **9**, (2016).
2. Chundawat, S. P. S. *et al.* Restructuring the crystalline cellulose hydrogen bond network enhances its depolymerization rate. *J. Am. Chem. Soc.* **133**, 11163–11174 (2011).
3. Gao, D. *et al.* Increased enzyme binding to substrate is not necessary for more efficient cellulose hydrolysis. *Proc. Natl. Acad. Sci.* **110**, 10922–10927 (2013).
4. Gomez Del Pulgar, E. M. & Saadeddin, A. The cellulolytic system of *thermobifida fusca*. *Crit. Rev. Microbiol.* **40**, 236–247 (2014).
5. Calza, R. E., Irwin, D. C. & Wilson, D. B. Purification and Characterization of Two B-1,4-Endoglucanase. *Biochemistry* **24**, 7797–7804 (1985).
6. Jalak, J., Kurašin, M., Teugjas, H. & Våljamä, P. Endo-exo synergism in cellulose hydrolysis revisited. *J. Biol. Chem.* **287**, 28802–28815 (2012).
7. Wilson, D. B. Cellulases of *Thermomonospora fusca*. *Methods Enzymol.* **160**, 314–323 (1988).
8. Bradford, M. M. A rapid and sensitive method for the quantitation of microgram quantities of protein utilizing the principle of protein-dye binding. *Anal. Biochem.* **72**, 248–254 (1976).
9. Gao, D. *et al.* Lignin triggers irreversible cellulase loss during pretreated lignocellulosic biomass saccharification. *Biotechnology for biofuels* **7**, (2014).
10. Ekperigin, M. M. Preliminary studies of cellulase production by *Acinetobacter anitratus* and *Branhamella* sp. *African J Biotechnol* **6**, 28–33 (2007).
11. Mandels, M. & Reese, E. T. Induction of Cellulase in *Trichoderma Viride* As Influenced By Carbon Sources and Metals. *J. Bacteriol.* **73**, 269–278 (1957).
12. Chen, S. & Wilson, D. B. Proteomic and transcriptomic analysis of extracellular proteins and mRNA levels in *Thermobifida fusca* grown on cellobiose and glucose. *J. Bacteriol.* **189**, 6260–6265 (2007).
13. Advisor, Y. D. & Fong, S. S. Characterization and genetic analysis of the cellulolytic microorganism *Thermobifida fusca*. (2011).
14. Novy, V., Schmid, M., Eibinger, M., Petrsek, Z. & Nidetzky, B. The micromorphology of *Trichoderma reesei* analyzed in cultivations on lactose and solid lignocellulosic substrate, and its relationship with cellulase production. *Biotechnol. Biofuels* **9**, 169 (2016).
15. Xiao, Z., Storms, R. & Tsang, A. Microplate-based assay to measure total cellulase activity. *Biotechnology and bioengineering* **88**, (2004).
16. Irwin, D. C., Spezio, M., Walker, L. P. & Wilson, D. B. Activity studies of eight purified cellulases: Specificity, synergism, and binding domain effects. *Biotechnol. Bioeng.* **42**, 1002–1013 (1993).
17. Chundawat, S. P. S. *et al.* Proteomics-based compositional analysis of complex cellulase-hemicellulase mixtures. *J. Proteome Res.* **10**, 4365–4372 (2011).
18. Henrissat, B., Driguez, H., Viet, C. & Schliebin, M. Synergism of Cellulases from *Trichoderma reesei* in the Degradation of Cellulose. *Nature Biotechnology* **3**, (1985).
19. Gao, D., Chundawat, S. P. S., Krishnan, C., Balan, V. & Dale, B. E. Mixture optimization of six core glycosyl hydrolases for maximizing saccharification of ammonia fiber expansion (AFEX) pretreated corn stover. *Bioresour. Technol.*

- 101**, 2770–2781 (2010).
20. Zhang, Y.-H. P., Cui, J., Lynd, L. & R Kuang, L. *A Transition from Cellulose Swelling to Cellulose Dissolution by o -Phosphoric Acid: Evidence from Enzymatic Hydrolysis and Supramolecular Structure*. *Biomacromolecules* **7**, (2006).
 21. A Whitehead, T., Bandi, C. K., Berger, M., Park, J. & Chundawat, S. *Negatively Supercharging Cellulases Render Them Lignin-Resistant*. *ACS Sustainable Chemistry & Engineering* **5**, (2017).